## Behavioral/Cognitive

# Model Sharing in the Human Medial Temporal Lobe

Leonie Glitz, Keno Juechems, Christopher Summerfield, and Neil Garrett<sup>1,2</sup>

<sup>1</sup>Department of Experimental Psychology, University of Oxford, Oxford OX2 6HG, United Kingdom, and <sup>2</sup>School of Psychology, University of East Anglia, Norwich NR4 7TJ, United Kingdom

Effective planning involves knowing where different actions take us. However, natural environments are rich and complex, leading to an exponential increase in memory demand as a plan grows in depth. One potential solution is to filter out features of the environment irrelevant to the task at hand. This enables a shared model of transition dynamics to be used for planning over a range of different input features. Here, we asked human participants (13 male, 16 female) to perform a sequential decision-making task, designed so that knowledge should be integrated independently of the input features (visual cues) present in one case but not in another. Participants efficiently switched between using a low-dimensional (cue independent) and a high-dimensional (cue specific) representation of state transitions. fMRI data identified the medial temporal lobe as a locus for learning state transitions. Within this region, multivariate patterns of BOLD responses were less correlated between trials with differing input features but similar state associations in the high dimensional than in the low dimensional case, suggesting that these patterns switched between separable (specific to input features) and shared (invariant to input features) transition models. Finally, we show that transition models are updated more strongly following the receipt of positive compared with negative outcomes, a finding that challenges conventional theories of planning. Together, these findings propose a computational and neural account of how information relevant for planning can be shared and segmented in response to the vast array of contextual features we encounter in our world.

Key words: model based; planning; reinforcement learning; RSA

#### Significance Statement

Effective planning involves maintaining an accurate model of which actions take us to which locations. But in a world awash with information, mapping actions to states with the right level of complexity is critical. Using a new decision-making "heist task" in conjunction with computational modeling and fMRI, we show that patterns of BOLD responses in the medial temporal lobe—a brain region key for prospective planning—become less sensitive to the presence of visual features when these are irrelevant to the task at hand. By flexibly adapting the complexity of task-state representations in this way, state-action mappings learned under one set of features can be used to plan in the presence of others.

## Introduction

Effective goal-directed behavior requires an agent to learn an accurate model of the world. Theories of reinforcement learning (RL) conceive of this model as a function, p(s'|s,a), that encodes

Received Oct. 1, 2021; revised Apr. 20, 2022; accepted Apr. 23, 2022.

Author contributions: L.G., K.J., C.S., and N.G. designed research; L.G. and N.G. performed research; L.G., C.S., and N.G. analyzed data; C.S. and N.G. jointly supervised this work; L.G., C.S., and N.G. wrote the paper.

This research was funded in part by the Wellcome Trust (Sir Henry Wellcome Postdoctoral Fellowship to N.G., Grant 209108/Z/17/Z), a European Research Council grant (ERC Consolidator Award: 725937) to C.S., support from the Human Brain Project (Special Grant Agreement No: 945539) to C.S. and a Waverley Scholarship to L.G. N.G. has applied a CC BY public copyright license to any author accepted manuscript version arising from this submission. The funders had no role in study design, data collection and analysis, decision to publish, or preparation of the manuscript. We thank Tania Martinez Montero and Alberto Sobrado for assistance with fMRI scanning. We also thank Dan Bang, for helpful insight and comments on an earlier draft of the manuscript; and Nathaniel Daw, for the expectation maximization code used for model fitting and comparison.

The authors declare no competing financial interests.

Correspondence should be addressed to Neil Garrett at n.garrett@uea.ac.uk or Leonie Glitz at leonie.glitz@psv.ox.ac.uk.

https://doi.org/10.1523/JNEUROSCI.1978-21.2022 Copyright © 2022 the authors

the probability of transitioning to a new state, s', given the current state, s, and action, a. Explicitly learning a state transition function permits agents to plan over possible futures (Sutton and Barto, 1998). This computational framework has been widely used to model simple laboratory behaviors that involve a limited number of state transitions (Gläscher et al., 2010; Daw et al., 2011; Wunderlich et al., 2012; Doll et al., 2015). However, it has well known limitations, foremost among which is that computational cost grows exponentially with the number of states.

One way that agents can reduce this computational cost is to selectively discard information, such as intervals of time (minutes, hours, days, etc.) and sensory cues, that can be used to segment experiences into separate states (Niv, 2019). For example, when planning a journey to work, travel delays when traveling by car (traffic jams), rail (train track repairs), or bike (getting wet) can all change from day to day. One way to reduce the cost of planning is to share knowledge of travel delays over multiple days where this is appropriate. For example, train delays might be invariant to whether one is traveling on a weekday or at the weekend.

Here, we developed an experimental paradigm that allowed us to test how the brain adapts the state representations it uses to plan efficiently. Our first question was whether participants would flexibly adapt how information was recruited and updated, switching between low-dimensional (cue-independent) and highdimensional (cue-specific) representations. Our question and approach here are similar to those described in a recent article by Baram et al. (2021), with a key difference being that our work examines how the transition function (how states of the world are associated), rather than the value function (the value of states and actions), is shared across or kept specific to the presence of different sensory cues. Our second question was posed at the neural level and addressed by recording fMRI data while participants performed the task. We focused on the medial temporal lobe (MTL), which has previously been shown to be important for forming new associations between states (Miyashita, 1988; Eichenbaum et al., 1999; Yokose et al., 2017; Rey et al., 2018) and involved in bridging past memories to make new inferences on the basis of paired associations or transitive relations (Bunsey and Eichenbaum, 1996; Wimmer and Shohamy, 2012; Zeithamova et al., 2012; Kumaran et al., 2016; Koster et al., 2018; Park et al., 2019). We find that a cluster of regions in the MTL, including the hippocampus, amygdala, and entorhinal cortex, display patterns of blood oxygenation level-dependent (BOLD) activity encoding transition probabilities that are more similar between sensory cues when model sharing is possible compared with when it is not. This suggests that the MTL maintains separable encoding patterns corresponding to each sensory cue in cases where state associations are cue specific, but uses a single cue-independent encoding pattern when they are not. Finally, we designed our paradigm such that the transition function (the probability of moving from s to s' under action a) and the value function (when in state s, the expected value of taking the action a that led to s') were theoretically independent. This allowed us to ask whether state transition learning depends on whether an outcome is positive or negative. We show that belief updating of state transition knowledge occurs to a greater degree following positive outcomes compared with negative. This learning asymmetry is reflected by an interaction in the MTL whereby state prediction errors (SPEs) are expressed with greater fidelity for positive compared with negative outcomes. These findings nuance conventional models of planning that assume state transitions and outcomes are tracked and maintained separately from one another.

## **Materials and Methods**

Participants. A total of 62 healthy volunteers with no self-declared history of psychiatric or neurologic disorders took part in the experiment. Thirty-one took part in the pilot experiment [18 female; mean (SD) age, 26.29 years (5.50 years)], and 31 participated in the main fMRI study. From the latter, two participants were subsequently excluded. One was excluded because their structural fMRI revealed a possible brain abnormality. A second participant was excluded because of excessive head motion (>10% of images contained motion artifacts on visual inspection). This left 29 participants (16 female; mean (SD) age, 25.86 years (3.59 years)] in the final sample. Participants were paid 10€/h plus a bonus contingent on performance.

Ethics statement. The fMRI study was approved by the ethics committee of the University of Granada where data collection was conducted. All participants gave written informed consent before scanning. The behavioral pilot was approved by the ethics committee at the University of Oxford where this dataset was collected. We obtained written informed consent from each participant.

Heist task. On each trial of the fMRI experiment, participants were presented with one of two doors (dark/light) on one (left/right) side of

the screen (side counterbalanced), in one of two "contexts" within the current block (Fig. 1a). Participants were instructed not to respond until an X appeared on the door. When an X appeared, on forced trials (24/ block), participants were required to select the door initially presented. On free-choice trials (8/block), participants could either choose the door initially presented or opt to choose the alternate door, which appeared on the opposite side of the screen also with an X (Fig. 1a). Participants had 1.5 s to respond; otherwise, the trial was aborted. Missed trials [mean (SD) = 6.41 (4.65)] were excluded from all analyses.

The selection of door influenced which of two possible second-stage states participants subsequently transitioned to. One of the doors transitioned with probability *p* to a heist state where participants could either win or lose money and transitioned with probability 1 - p to a neutral state in which participants would always receive 0 as an outcome (participants were only rewarded for free-choice trials). The alternate door transitioned to the same second-stage states but with the inverse probability (i.e., probability 1 - p of transitioning to the heist state and probability p to the neutral state; Fig. 1b). The value of p was set to either 0.2 or 0.8, alternating randomly between these two values throughout the task (with probability of changing equal to 0.1 on every trial). This meant that one door was always likely to transition to one of the outcome states and unlikely to transition to the other. Participants were told state transitions could change, but were not told the probability with which this could happen. Importantly, p always had the same value for both contexts in dependent blocks. In independent blocks, the values for p were independent in the two contexts. Participants were explicitly told this probability structure during the instructions and the block type they were in (dependent/independent) was clearly signaled to them at the start of a new block of trials. The context of the current trial was signaled to participants by the color of a gemstone presented in the center of the screen (green, yellow, blue, or red). The assignment of gemstone to context was different for each participant but (after assignment) remained the same throughout the experiment. Alongside this contextual cue, during door and response presentation participants were also shown a stimulus (either swag bag or police) indicating whether they would receive a gain (if a swag bag was shown) or incur a loss (if police were shown) if they reached the heist state (this changed randomly on every trial). They were also shown a sofa stimulus, which indicated they would get 0 on reaching the sofa state (this was the case in every trial). Since whether a gain or loss was possible in the heist state was signaled to participants (and alternated on each trial), this meant that participants should aim to reach the heist state on 50% of trials (when the swag bag was presented) and aim to avoid this state (i.e., reach the sofa state) on the remaining 50% of trials (when the police were shown). Explicitly providing participants with this information was done to remove the need to actively learn the value of each bottom-level state, emphasize the need to track the transition function, and use current beliefs about this function to plan. After indicating their choice, participants were shown the state they transitioned to and the resulting outcome—either a gain or a loss if they transitioned to the heist state (depending on whether the police or swag bag stimuli had been presented at the time of choice) or zero if they transitioned to the neutral state.

The task took place in sessions of trials (two blocks of 32 trials/ session, five sessions total during the experiment, and 320 trials total). The first session took place outside of the scanner. Each session contained one block of trials in the dependent condition and one block of trials in the independent condition. The order of the blocks was counterbalanced across sessions. Participants indicated their response using a computer keyboard (outside the scanner) or MRI-compatible button box (inside the scanner). Participants were paid a base rate bonus of 2.50€ plus 2.5 times their percentage of correct free-choice trials (up to 5€ total). The task was programmed in MATLAB using Psychtoolbox (Kleiner et al., 2007).

Behavioral analysis (adapting information integration between contexts). To examine the extent to which participants updated beliefs about state transitions within and between contexts, logistic regression analyses were conducted [mixed-effects models using the fitglme fitting routine in MATLAB, version 2020 (https://www.mathworks.com/)]. Models tested to what extent subjects' choice behavior on each trial (coded as: select dark

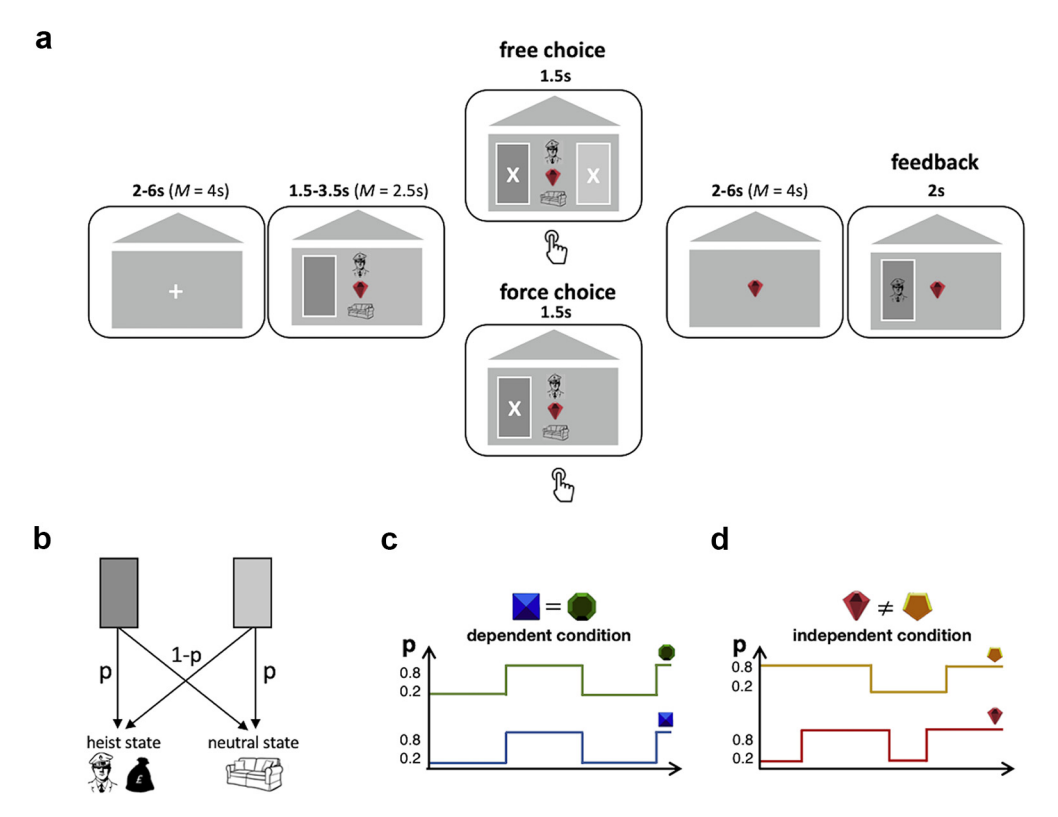


**Figure 1.** Task design.  $\boldsymbol{a}$ , Trial sequence in the fMRI experiment. Each trial begins with a fixation cross after which participants are shown one of two options (a dark and a light door) along with one of four contextual cues (red gem in the example) and two stimuli (sofa plus either police or swag) indicating the outcome if they transition to the heist state (if police shown, -1; if swag shown, +1) or the neutral state (always sofa = 0). In forced-choice trials (75% of trials), participants are then required to select this option via a button press. In free-choice trials (25% of trials), they can choose between this option and the alternate option. Participants were instructed to respond when an X appeared on one or both doors. Feedback—the subsequent state along with the outcome—is then revealed.  $\boldsymbol{b}$ , State transition dynamics: at the first stage, each option (framed as two doors) transitions participants to one of two second-level states; a neutral state in which an outcome of 0 (sofa/chair stimuli) is always obtained or a heist state in which an outcome of 1 (swag bag stimuli) or -1 (police stimuli) can be obtained (note which of these two outcomes will be obtained at the heist state is signaled to participants in advance by the presence of one of these cues at choice). One first-stage option (light door in the figure) transitions with probability p to the neutral state and with probability 1-p to the heist state; the alternate option (dark door) has the opposite transition probabilities. p changes at random points in the task. q, In independent blocks (not real data), p alternates independently in each context. q was set to be either 0.2 or 0.8 at any given time.

door = 1; select light door = 0) was influenced by transitions experienced over the previous five trials.

To examine this, we first constructed five variables that coded the evidence received from the state transition n trials back (relative to the current trial t), where n ranged from 1 to 5. When trial t was a gain trial, previous transitions to the heist state were coded 1 (-1) if the dark (light) door was selected t - n trials back and participants transitioned to the heist state, and coded -1 (1) if the transition encountered was to the neutral state. This coding was reversed for loss trials (Fig. 2). The intuition implicit in this coding scheme is that participants would aim to repeat choices that previously transitioned to the heist state on gain trials but to switch choices on loss trials (in an attempt to transition to the neutral state and avoid incurring a loss). We also partitioned trials according to whether evidence was received in the same or alternate context as the current trial t. This led to a total of 10 variables—5 encoding evidence received one to five trials back from the same context and 5 encoding evidence received one to five trials back from the alternate context. A "0" was entered as a value for cases where a variable did not apply for a particular trial (e.g., if three trials back a subject's choice was executed in the alternate context, evidence three trials back in the same context would be assigned a value of 0 for this trial).

Next, to assess qualitatively whether the degree of information integration from each context (same and other) changed between conditions, we entered all 10 variables in separate mixed-effects models: one for the dependent condition and one for the independent condition. Only choices from free-choice trials were entered in the model as the dependent variable (however, the information encoded in the independent variables used to predict choice could come from free or forced trials as

participants could use transition information from both trial types). All regressors and the intercept were taken as random effects (i.e., allowed to vary across subjects).

The model was specified in the syntax of the MATLAB fitglme routine as follows:

$$\label{eq:DarkDoor} \begin{split} \operatorname{DarkDoor} &\sim \operatorname{oneBackSame} + \operatorname{twoBackSame} + \operatorname{threeBackSame} \\ &+ \operatorname{fourBackSame} + \operatorname{fiveBackSame} + \operatorname{oneBackOther} \\ &+ \operatorname{twoBackOther} + \operatorname{threeBackOther} + \operatorname{fourBackSame} + \operatorname{twoBackSame} \\ &+ \operatorname{fiveBackSame} + \operatorname{fourBackSame} + \operatorname{fiveBackSame} \\ &+ \operatorname{oneBackOther} + \operatorname{twoBackOther} + \operatorname{threeBackOther} \\ &+ \operatorname{fourBackOther} + \operatorname{fiveBackOther} | \operatorname{subject}) \end{split}$$

To the extent that participants are using information from each context to a similar degree (which ought to be the case in dependent blocks), coefficient estimates ought to have a similar magnitude for same and other context. To the extent that participants ignore information from an alternate context (which ought to be the case in independent blocks), there ought to be separation between coefficient estimates from same versus other. Note that by controlling multiple trials back, we guard against the possibility that information used in the alternate context can have an effect in the dependent condition by virtue of the fact the feedback received is similar in the two contexts.

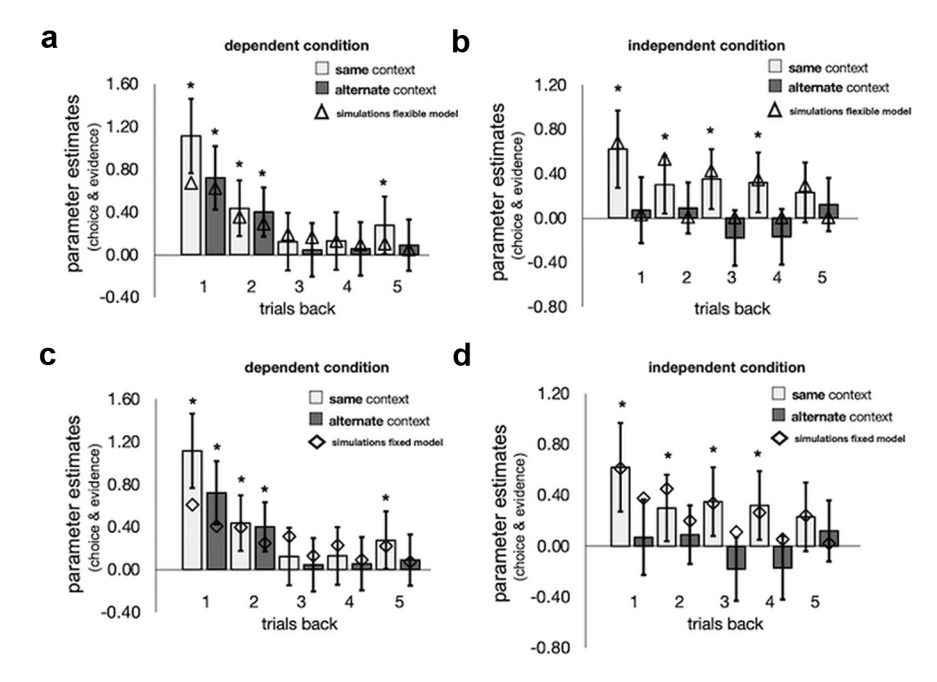


**Figure 2.** Behavioral data. a, b, Parameter estimates predicting choice from state transitions experienced one to five trials back, separated according to whether transitions occurred in the same (blue) or alternate (red) context to the current trial context in the dependent condition (a) and the independent condition (b). Bars represent fixed-effects regression coefficients from a mixed-effects logistic regression on participants' choices. Triangles represent the mean fixed-effects regression coefficient estimates generated via the same mixed-effects logistic regression as the data but for choice simulated for agents under a flexible computational learning model, which enables evidence integration to adapt to the condition in which choices are being made (dependent or independent). c, d, Plot the same parameter estimates with simulated agents from the fixed learning model (in diamonds), which does not permit adaptation in evidence integration. \*p < 0.05 (human data). Error bars express 95% confidence intervals.

Finally, to assess quantitively whether differences in information integration between conditions were significant, we averaged the streams of evidence of each condition for picking the dark door on the current trial over the past five trials. This resulted in the following two quantities:

$$average\_evidence\_Same = (oneBackSame + twoBackSame \\ + threeBackSame + fourBackSame \\ + fiveBackSame)/5$$
 
$$average\_evidence\_Other = (oneBackOther + twoBackOther \\ + threeBackOther + fourBackOther \\ + fiveBackOther)/5$$

We then subtracted average\_evidence\_Other from average\_evidence\_Same providing the following difference score:

$$\label{eq:differential_evidence} \begin{split} differential\_evidence = & average\_evidence\_Same \\ & - average\_evidence\_Other \end{split}$$

The differential evidence score reflects a relative preference in updating beliefs for information received from the same context over information received from the other context. When equal to 0, individuals are indifferent between evidence from the same and evidence from the other context. When >0, individuals prefer (i.e., update beliefs to a greater degree) information received in the same context compared with the other context. When <0, individuals prefer information received in the other context compared with the same context.

We used this differential evidence score in a third mixed-effects model to test whether preferences for the context in which information was received shifted with condition (captured in the model as a Differential Evidence by Condition interaction). The model was specified as follows: DarkDoor ~ differential\_evidence

- \* Condition
- $+(1 + differential\_evidence$
- \* Condition|subject).

Condition was again coded as 1 = Dependent condition, -1 = Independent condition.

Computational model. Our model is not intended primarily as an account of the computations that humans undertake, but as an analytic tool. Participants are assumed to track the underlying state transition structure of the task in the form of p, an estimate of the probability that selection of one of the two doors (which of the two is arbitrary, but in our modeling this is taken to be the dark door) transitions to the heist state. This is assumed (as is the actual case in the experimental design) to be equal to the probability that the alternate door transitions to the neutral state. It is also assumed (as is the case) that 1 - p is equal to the probability of each door going to the alternate state (dark goes to neutral and light to heist). Under these assumptions, maintaining a belief about a single quantity, p, enables computation of estimates for each door going to each second-level (terminating) state. Importantly, participants are assumed to maintain the following two sets of beliefs about p:  $p_{\text{specific}}^{i}$ and  $p_{\text{independent}}$ .  $p_{\text{specific}}^{i}$  maintains separate estimates of p, exclusive to each context where i indexes the two contexts in each block (i.e.,

 $[p_{\rm specific}^{i=1},\ p_{\rm specific}^{i=2}]).\ p_{\rm independent}\ {\rm maintains}\ {\rm a}\ {\rm single}\ {\rm estimate}\ {\rm of}\ p,$  which updates across contexts (within the same block). All estimates of p were initialized to 0.5 at the start of the experiment in all models. Estimates of p were allowed to carry over between blocks (i.e., p did not reset to 0.5 at the start of a new block).

At the time of choice, participants then combine the two sets of beliefs  $(p_{\text{specific}}^i, p_{\text{independent}})$  into a single estimate,  $\hat{p}_c$ , according to the following:

$$\hat{p}_c = w * p_{\text{independent}} + (1 - w) * p_{\text{specific}}^i$$

We tested a baseline model in which w was held fixed between conditions. We refer to this as the fixed model. We tested this against a second model, which was identical in all respects except that it allowed w to reverse in the independent condition. In other words, in the dependent condition,  $\hat{p}_c$  was calculated as follows:

$$\hat{p}_c = w * p_{\text{independent}} + (1 - w) * p_{\text{specific}}^i$$

In the independent condition.  $\hat{p}_c$  was calculated as follows:

$$\hat{p}_c = (1 - w) * p_{\text{independent}} + w * p_{\text{specific}}^i$$

We refer to this as the flexible model.

In both models, combined estimates of  $p(\hat{p}_c)$  were then used to calculate the value of selecting each door, as follows:

$$Q_{\text{dark door}} = r * \hat{p}_c$$

$$Q_{\rm light\,door} = (r*1 - \hat{p}_c),$$

[r=1 on gain trials, -1 on loss trials].

Following choice, after participants observed the second-level state they transitioned to, a state prediction error,  $\delta$ , was calculated as follows:

$$\delta = x - \hat{p}_{c}$$

[x=1] if chose dark door and transition to heist state OR chose light door and transitioned to neutral state; x=0 if chose dark door and transitioned to neutral state OR chose light door and transitioned to heist state].

This prediction error was then applied to update both sets of beliefs about p, as follows:

$$p_{\text{independent}} = p_{\text{independent}} + w * \alpha * \delta$$
,

$$p_{\text{specific}}^{i} = p_{\text{specific}}^{i} + (1 - w) * \alpha * \delta.$$

Where the context indexing  $p_{\text{specific}}^i$  can be context 1 or context 2. The w used in each update is identical to the w used to compute  $\hat{p}_c$ 

The w used in each update is identical to the w used to compute  $\hat{p}_c$  and was either held fixed (fixed model) or allowed to reverse between conditions (flexible model).

To avoid probability estimates exceeding 1 or going <0 (which in a small number of cases is possible in this setup), updates to beliefs were bounded to within this range.

The probability of choosing the dark door was then estimated using a softmax choice rule, as follows:

$$p(\mathsf{choice} = \mathsf{dark}\,\mathsf{door}) = \frac{1}{1 + \exp\Bigl(\beta \left(Q_{\mathsf{light\_door}} - Q_{\mathsf{dark\_door}}\right)\Bigr)} \,.$$

Altogether, each model has the following three parameters:  $\alpha$ ,  $\beta$ , and w. For each participant, we estimated the free parameters of the model by maximizing the likelihood of their sequence of choices, jointly with group-level distributions over the entire population using an expectation maximization (EM) procedure (Huys et al., 2011; Garrett and Daw, 2020), which maximizes the joint likelihood of each participant's sequences of choices where each individual's parameter estimates are random effects drawn from group-level Gaussian parameter distributions whose means and variances and also estimated) implemented in the Julia language (version 0.7.0; Bezanson et al., 2012). Note that, similar to the behavioral analysis reported above, all trials (forced and free) were included in the model but only free-choice trials were included in the likelihood calculation. Models were compared by first computing unbiased per subject log marginal likelihoods (using the Laplace approximation) via subject-level cross-validation (iteratively holding out each subject and estimating the free parameters of the model for the remaining participants using the EM optimization algorithm then using these estimates as a Gaussian before optimizing the left-out subject choices) and then comparing these likelihoods (one per participant) between models (Flexible vs Fixed) using paired sample t tests (two sided).

Computational simulations. To examine the qualitative fit of each learning model to the data, we ran separate simulations for the Fixed Model (in which w was held constant across conditions) and the Flexible Model (in which w was allowed to vary with condition). For each simulation (n = 504 for each model), we ran a group of 29 virtual participants. For each virtual participant, we randomly selected (with replacement) a set of parameters ( $\beta$ ,  $\alpha$ , and w) from the best fit parameters generated by the computational model (fit to actual participants choices). We then simulated the learning process by which estimates of p evolved (given door selection and state encountered), exactly as described for the respective computational models. To mimic the task as closely as possible, 25% of virtual agent trials were free-choice trials in which we simulated which of the two doors were selected (given current beliefs about p, and whether a gain or a loss was available in the heist state), and 75% were forced-choice trials where the door selected was chosen for them (as a coin flip).

We then entered choices made by each virtual agent as the dependent variable in a binomial mixed-effects model with regressors coding evidence received one to five trials back from the same and alternate context (10 regressors in total). This was run separately for each condition, replicating the analysis conducted on the data (i.e., actual subjects'

choices) with the same model specification (as before, all regressors and the intercept were taken as random effects). This generated a set of fixed-effect parameter estimates for each simulation for each condition. We then averaged each fixed parameter estimate over the simulations and compared these to the parameter estimates generated from the data.

Finally, we used the fixed model to run a permutation test to estimate the extent to which an interaction between differential evidence and condition (our third mixed-effects model) could arise under agents that did not change information integration between contexts that might occur because of feedback being more similar in the dependent condition compared with the independent condition. Specifically, we simulated choices for 500 groups made up of 29 agents each in performing the task. For each agent, we randomly selected (with replacement) a set of parameters  $(\beta, \alpha)$  from the best fit parameters generated by the fixed model (fit to actual participants choices). w could take any value between 0 and 1 (uniformly distributed) and could not reverse between contexts. For each group, we then calculated differential evidence scores on each trial for each participant and entered these into a mixed-effects model to predict choices (along with condition and their interaction) exactly as we did using participants' data. This generated a distribution of fixed-effects estimates and t statistics that we used to calculate a 95% confidence interval (CI) and compare against the estimates found in the data.

fMRI image acquisition, preprocessing and reporting. MRI data were acquired on a 3T Magnetom Trio MRI Scanner scanner (Siemens). A whole-brain, high-resolution, T1-weighted anatomical structural scan was collected before participants commenced the four in-scanner blocks of the task (imaging parameters: voxel resolution = 1 mm<sup>3</sup>; TR = 1900 ms; TE = 2.52 ms; TI = 900 ms; slice thickness = 1 mm; voxel resolution = 1 mm<sup>3</sup>). During the task, axial echoplanar functional images with BOLD-sensitive contrast were acquired in descending sequence (imaging parameters: 32 axial slices per image; voxel size = 3.5 mm<sup>3</sup>; slice spacing = 4.2 mm; TR = 2000 ms; flip angle =  $80^{\circ}$ ; TE = 30 ms). The 462 volumes were collected per participant per session (total number of volumes over the four sessions = 1848), resulting in a scanning time of  $\sim$ 1 h. Image analysis was performed using SPM12 (http://www.fil.ion. ucl.ac.uk/spm). The following procedures were used for preprocessing of the raw functional files. Slice-time correction referencing was applied with reference to the middle slice to correct for/avoid interpolation errors because of the descending image acquisition sequence (Juechems et al., 2017, their reference Sladky et al., 2011). Then, realignment of the images from each session with the first image within it was performed. The crosshair was adjusted to the anterior commissure manually to improve coregistration. After coregistration of the functional with the structural images was performed, segmentation, normalization, and smoothing of the .epi files was undertaken. We then checked for motion artifacts and flagged scans as well as warping manually.

In all fMRI analyses [univariate and representational similarity analysis (RSA) searchlights], we report activation that survives small volume correction at peak level within an anatomical or functional region of interest (ROI) mask (see below for how these were defined). Other brain regions were only considered significant at a level of p < 0.001 uncorrected if they survived whole-brain familywise error (FWE) correction at the cluster level (p < 0.05).

Anatomical masks. Anatomical masks were generated using the automated anatomic labeling atlas (Tzourio-Mazoyer et al., 2002) and Talairach Daemon Atlas (Lancaster et al., 2000), which was used to define Brodmann area 28 as entorhinal cortex (Canto et al., 2008) and Brodmann area 17 as V1 (Tootell et al., 1998) integrated into the WFU Pickatlas graphical user interface (GUI; Maldjian et al., 2003), as follows: (1) a bilateral medial temporal lobe mask used for small-volume correction, which was defined as including the bilateral hippocampus, entorhinal cortex, parahippocampus, and amygdala, and dilated by a factor of 1 in the WFU Pickatlas GUI; (2) bilateral amygdala (84 voxels), hippocampus (336 voxels), entorhinal cortex (53 voxels), and parahippocampus (404 voxels) masks (no dilation) used for anatomical definition of our ROI from fMRI general linear model (GLM) 1 (see below) as well as post hoc RSA tests (see Fig. 4); and (3) bilateral V1 (121 voxels) and bilateral primary motor cortex (Brodmann area 4, 240 voxels) used as a control region for the post hoc RSA tests (see Fig. 4).

All masks were resliced to match the dimensions of our data using the SPM fMRI Realign (Reslice) function.

fMRI general linear model 1. For each participant, the BOLD signal was modeled using a GLM with time of door presentation and time of outcome presentation as onsets. Events were modeled as delta (stick) functions (i.e., duration set to 0 s) and collapsed over our two experimental conditions (dependent and independent blocks).

To identify brain regions that tracked state prediction errors, we extracted trial by trial estimates of unsigned state prediction errors,  $|\delta|$ , from our computational model and entered these as parametric regressors, modulating the time of outcome for each participant. In addition, we also entered the following regressors: outcome received (1, 0, or -1), the interaction of outcome with unsigned state prediction error (i.e., the product of outcome received with  $|\delta|$  on each trial) and trial type (1 = forced, -1 = free). Six movement parameters, estimated from the realignment procedure were added as regressors of no interest.

ROI definition. We identified regions in which the BOLD response was parametrically modulated by the magnitude of the unsigned state prediction error ( $|\delta|$ ), using a threshold of p < 0.001 uncorrected, with cluster size > 10 voxels. Clusters identified were saved as binary ROIs (in SPM) and then combined into a single ROI using the MarsBaR toolbox (http://marsbar.sourceforge.net/). This functional ROI was then used for a subsequent RSA (see below). We divided the number of voxels that fell within both our functional ROI and each anatomical mask by the total number of voxels in our functional ROI. This gave us the percentage with which our functional ROI was a conjunction of each anatomical region.

fMRI GLM 2a (door presentation). For each participant, we created a design matrix in which each door presentation (32 per condition per session) was modeled as a separate event (without parametric regressors attached). Such a procedure has been used multiple times in the past (Charpentier et al., 2014; Garrett et al., 2016). Outcome onset was entered as an additional event. Events were modeled as delta functions and convolved with a canonical hemodynamic response function to create regressors of interest. Six motion correction regressors estimated from the realignment procedure were entered as covariates of no interest.

RSA (door presentation). To examine whether BOLD responses were more similar between contexts in the dependent versus independent condition, we used GLM2a to extract estimates of BOLD response on each trial in our functional ROI (identified from GLM 1) and partitioned these estimates into four linearly spaced bins according to how likely the door presented was to go to the heist state ( $P(\text{state} = \text{heist} \mid \text{door presented})$ ). This was inferred by extracting a trial by trial estimate of  $p_{\text{combined}}$  (from the flexible learning computational model) and using  $p_{\text{combined}}$  or  $1 - p_{\text{combined}}$  depending on whether the dark or light door was presented, respectively, to estimate  $p(\text{state} = \text{heist} \mid \text{door presented})$ .

We divided trials into quartiles based on p(heist state | door presented), resulting in the following average (SD) probability bins: Bin 1, 0.04 < p (heist state | door presented)  $\leq 0.21$  (0.10); Bin 2, 0.21 < p (heist state | door presented)  $\leq 0.51$  (0.09); Bin 3, 0.51 < p (heist state | door presented)  $\leq 0.80$  (0.09); and Bin 4, 0.80 < p (heist state | door presented)  $\leq 0.96$  (0.03).

This was done separately for each context that the participant (N=29) encountered (2 in dependent blocks and 2 in independent blocks, 16 bins in total). We then averaged these estimates in each voxel in our functional ROI (collapsing across the four functional runs) for each bin generating an average BOLD response for each voxel.

To compare the similarity of responses between contexts, we proceeded by first calculating the dissimilarity of BOLD responses in each of the four bins between contexts. We computed this using (Pearson) correlation distance (using the pdist function in MATLAB); hence, high correlation indicates a low level of dissimilarity (conversely a high level of similarity). This generated an  $8\times 8$  dissimilarity matrix for each condition of which we subselected the  $4\times 4$  matrix displaying the dissimilarity of probability bins between the two contexts [i.e., context 1 vs context 2 for each level of p (heist state | door presented).

Dissimilarity scores were then converted into similarity scores (high scores indicating greater similarity) and Fisher transformed to allow

inference at the group level. The four similarity scores along the diagonal of each RSA matrix (where identical bins are compared between contexts) were averaged for each participant, creating an on-diagonal similarity score that quantifies the extent to which identical values of transition probabilities are encoded similarly between the two contexts in a condition. The 12 similarity scores on the off-diagonal of each RSA matrix (where different bins are compared between contexts) were separately averaged together to create off-diagonal similarity scores. Note that, unlike in regular RSA analyses, all 12 scores were averaged across rather than just the upper or lower triangular as the values in the  $4 \times 4$ matrix are not identical about the diagonal (off-diagonal 4×4 of a larger  $8 \times 8$ ; see above). We then computed the difference between ondiagonal and off-diagonal scores separately for each condition. Onesample t tests (vs 0) were conducted to assess whether significant differences between on-diagonal and off-diagonal similarity scores existed. Two-tailed paired sample t tests were used to compare whether difference scores were greater for the dependent condition compared with the independent condition.

The same RSA procedure was applied to voxels within the four anatomical ROIs used to characterize the nature of the effect within the medial temporal lobe and the control regions V1 and M1 (see Fig. 4). The interaction ANOVA result reported in the text are Greenhouse–Geisser corrected to adjust for violations of sphericity (both F value and degrees of freedom).

To check whether there is a relationship between the temporal proximity of trials between contexts and how similar the neural patterns are, we calculated the mean temporal distance between trials in the two contexts on the diagonal and the off-diagonal in each condition for each participant. We then correlated the difference in proximity between diagonal and off-diagonal trials with the difference in representational similarity between the diagonal and off-diagonal in the dependent and the independent condition.

Encoding model analysis. As a complementary approach, we built a linear encoding model, equivalent to a cross-validated multinomial logistic regression, that mapped voxels (within an ROI) onto probabilities under different constraints. We evaluated this model in cross-validation, using independent held-out data from across scanner runs. Briefly, we first extracted single-trial estimates of BOLD within the MTL ROI for each gem on each session, yielding data Y of size  $v \times t$ , where v is the number of voxels and t is the number of trials on which that gem was presented. We also recoded (scalar) single-trial, model-derived estimates of transition probability (converted to odds ratios) as input vectors in either a one-hot format (i.e., a 1 within the relevant bin and zeros elsewhere) or a Gaussian format (i.e., a Gaussian tuning curve that was maximal in the relevant bin but gradually tapered over adjacent bins). We used n bins falling within the range (in log odds) units of -2 to 2, where n varied exhaustively from 1 to 10. This yielded data X of size  $n \times t$ . We estimated weights w by linear regression of  $X_i$  onto  $Y_i$  for scanner run i and evaluated the fit of the model to held out probabilities  $X_i$ from multivariate patterns  $Y_i$  acquired in scanner run j. We used a (mean) cross-entropy loss in validation. This exercise allowed us to verify, for each gem, the cross-validated loss when weights obtained with gem g were evaluated with gem g' with which it co-occurred, both in the independent condition (where the probabilities were different) and the dependent condition (where they were not). We tested whether there was stronger cross-validation between gems (and across runs) in the dependent than the independent condition, for a varying number of bins nand with both one-hot and Gaussian input functions.

Searchlight RSA (door presentation; whole-brain). To assess whether our ROI was the only brain area with dependent and independent block transition probability representations and potential differences between them or whether this representation was distributed across the brain (and thus potentially less meaningful), we also conducted a whole-brain searchlight analysis. The searchlight analysis was conducted using a combination of scripts from the RSA toolbox (Nili et al., 2014) and our own parser script feeding in the single-trial onset events generated in GLM2a. The searchlight radius used was 10.5 mm (corresponding to 3 voxels). Neural representational dissimilarity maps for the two block types were

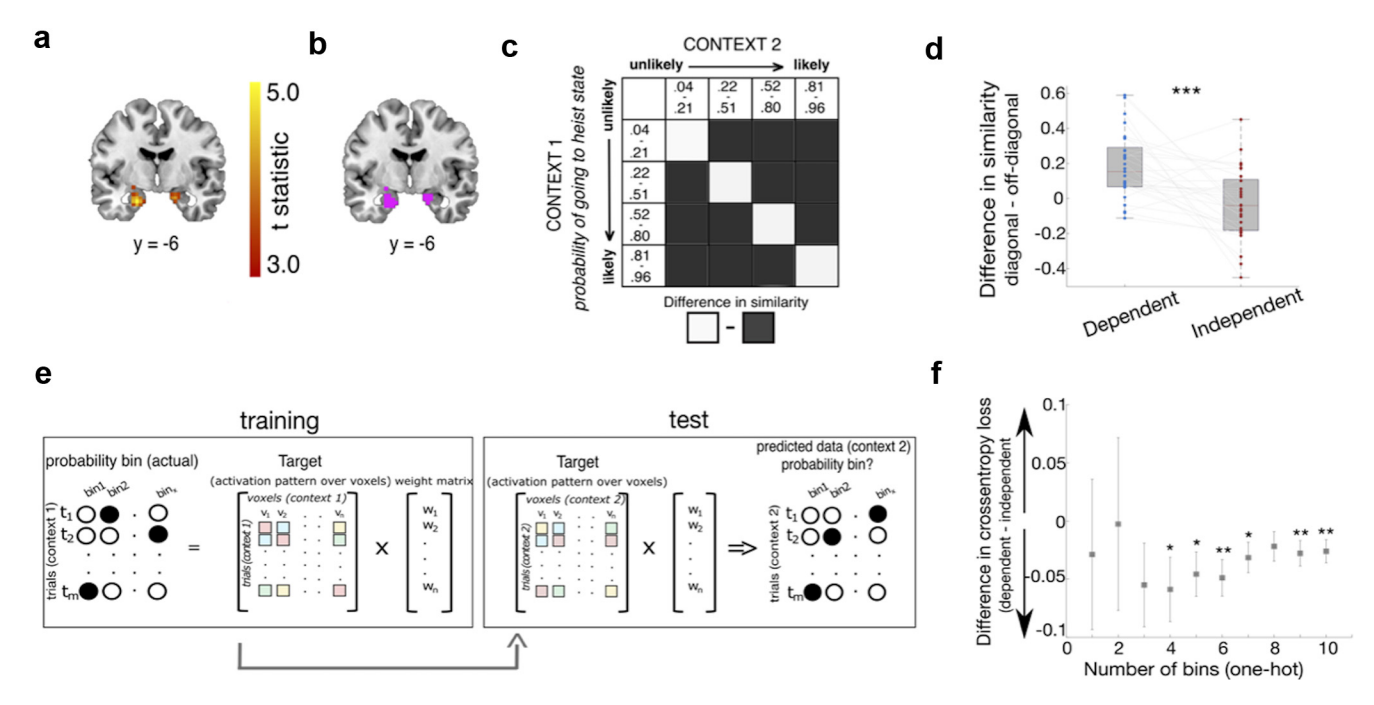


**Figure 3. a**, The magnitude of (unsigned) state prediction errors related negatively to the degree of BOLD response in bilateral MTL. Image shown at p < 0.001 uncorrected. **b**, Voxels in this contrast were converted to a bilateral mask and used as a functional ROI in subsequent analysis. **c**, Schematic of the RSA at the time of planning (door presentation). In each context, trials were divided into quartiles, according to participants' current estimates of p (heist state | door presented) extracted from the computational learning model (mean quartile ranges: bin 1,  $p \le 0.21$ ; bin 2, 0.21 ; bin 3, <math>0.51 ; bin 4, <math>0.80 ).**d**, Difference scores were significantly greater for dependent than independent blocks. Dots represent individual participant data, gray lines indicate datapoints belonging to the same participant. Red line indicates the median, box represents the 25th and 75th percentile of data, and whiskers extend to any data point that is not outside 1.5 times the interquartile range.**e**, Schematic of the encoding model analysis (example shown for one-hot case).**f**, Difference in cross-entropy loss from the encoding model between dependent and independent blocks (predicting probability bins in one context in a condition using weights trained on the other context in that condition; in cross-validation) for a range of probability bins (one-hot case). Error bars show SEM. \*significant at <math>p < 0.05; \*\*significant at p < 0.01; \*\*\*significant at p < 0.001.

separately correlated with model representational dissimilarity matrices (RDMs) using Spearman's correlation coefficient. The model RDM specified that the on-diagonal was more similar between contexts than the off-diagonal. This was done individually for each participant, and the resulting maps of correlation coefficients were saved. Second-level analysis as described above was then applied to the r-maps to establish separate group-level effects for the two conditions (i.e., the dependent and independent blocks). We report any brain regions that survive whole-brain correction at the cluster level after thresholding at p < 0.001.

fMRI GLM 2b (outcome presentation). For each participant, we created a design matrix in which each outcome presentation (32 per condition per session) was modeled as a separate event (without parametric regressors attached). Door presentation onset was entered as an additional event.

RSA (outcome presentation). We used GLM2b to extract estimates of BOLD response on each trial in our functional ROI and partitioned these estimates into bins according to the combination of doors chosen and state encountered. These combinations (of which there are four in total) drive the direction and degree of update of beliefs (p) about state transitions in the computational model. Specifically, we divided responses into bins as follows: Bin 1, dark door chosen + heist state encountered; Bin 2, dark door chosen + neutral state encountered; Bin 3, light door chosen + heist state encountered; and Bin 4, light door chosen + neutral state encountered.

This was done separately for each context that the participant encountered (2 in dependent blocks and 2 in independent blocks, 16 bins in total). We then averaged these estimates in each voxel in our functional ROI (collapsing across the four functional runs) for each bin generating an average BOLD response for each voxel.

To compare the similarity of responses between contexts, we followed a similar procedure to the RSA conducted at door presentation. We first calculated the dissimilarity of BOLD responses in each of the four choice–outcome state combinations across the two conditions generating 2 separate 8  $\times$  8 disimilarity matrices, of which we subselected the off-diagonal  $4\times 4$  for further analyses (context 1 vs context 2 for

each of the four choice–outcome state combinations computed separately for each condition). After conversion to similarity scores and Fisher transformation, the 4 on-diagonal similarity scores and the 12 off-diagonal similarity scores of each RSA matrix were averaged to create two sets of similarity scores per condition. The mean on-diagonal and off-diagonal similarity scores were then entered into a paired t test to assess differences between identical choice–outcome bins and nonidentical choice–outcome bins in the two contexts. Then, to assess whether there were meaningful differences between conditions, the difference between the mean on-diagonal and off-diagonal scores for each participant in each condition was entered into a paired t test (dependent on-diagonal–off-diagonal):

The same RSA procedure was applied to voxels within the four anatomical ROIs used to characterize the nature of the effect within the medial temporal lobe and the control regions V1 and M1. Again, the ANOVA results reported were Greenhouse–Geisser corrected because of violations of the assumption of sphericity.

Searchlight RSA (outcome presentation; whole-brain). The searchlight analysis was implemented in the same way as described above for the searchlight RSA at time of door onset. Here, the onset events read into the searchlight script were the outcome onset events generated in GLM2b. Again, the model RDMs specified that the on-diagonal (identical choice-outcome combinations for the two contexts within a condition) was more similar than the off-diagonal (see Fig. 5a) and that the analysis was conducted separately for the two conditions.

Searchlight interaction analysis (outcome presentation; whole-brain). The interaction analysis was also conducted similarly to the analysis described above for the time of door onset. In this case, if there is a difference between the difference scores for the two conditions, this means that the difference between the similarity in encoding of identical choice—outcome combinations and different choice—outcome combinations across the two contexts is different between the two conditions. If this difference is positive (as this analysis is coded as encoding similarity), it means the same choice—outcome combinations are encoded more

similarly between contexts than nonidentical choice–outcome combinations in dependent than in independent blocks and vice versa if this difference is negative. As for door presentation, we report any brain regions that survive whole-brain correction at the cluster level after thresholding at p < 0.001.

fMRI general linear model 3. To visualize the parametric effect of our interaction term ( $|\delta|$  \* outcome) in GLM1, we ran a separate GLM that included onsets of door presentation and outcome presentation with outcome onsets separated into the following three separate events: outcome presentation when participants received an outcome of +1, outcome presentation when participants received an outcome of 0, and outcome presentation when participants received an outcome of -1. Each of the three outcome onsets was modulated by two parametric regressors: unsigned state prediction error (extracted from our flexible RL model); and trial type (force/free). Events were modeled as delta functions and collapsed over our two experimental conditions (dependent and independent blocks), just as for fMRI GLM1. Six movement parameters, estimated from the realignment procedure, were added as regressors of no interest. We then extracted the parametric betas for the state prediction error regressors for each participant from the three outcome conditions using the MarsBaR toolbox at the peak voxel of the  $|\delta|$ \* outcome cluster identified in GLM1.

Participants and task (behavioral pilot). Thirty-one self-declared healthy individuals (18 female; mean = 26.29 years; SD = 5.50) were recruited using opportunity sampling via the Oxford University Research Recruitment System. The task was the same as the fMRI cohort undertook, as described above) save for the following differences. First, participants performed eight blocks of 60 trials (480 trials total), and all trials in this design were free-choice trials. This provided us with a higher-powered design to detect differences in updating because of outcome received at the end of an episode. After an intertrial interval (0.3–0.5 s), participants had up to 5 s to make their choice, after which they received confirmation of their choice (0.5 s) and feedback (1 s). Second, participants were not informed about the differences between blocks. However, just as before, each block had two different contexts: a dependent block in which transitions for the two contexts were the same and an independent block in which the transitions were independent.

Behavioral analysis (outcome valence and state transition updating). To examine the effect of outcome valence on transition updating, we calculated a consistency score for each participant. This is the percentage of times a participant's choices were consistent given both of the following: (1) the previous trials state-action-state sequence; and (2) whether the current trial was a gain or a loss trial. Since the same state-action-state sequence can lead to repeating or switching being the correct thing to do—depending whether the next trial is a gain or a loss trial—we first divided trials into two types, repeat and switch. Repeat trials are those for which participants would want to revisit the terminating state from the previous trial. For example, participants would want to repeat their choice if they picked the gray door on the last trial, went to the heist state and the next trial is a gain trial. These trials comprised the following: (1) trials where they previously reached the heist state and the current trial was a gain trial; and (2) trials where they previously reached the neutral state and the current trial was a loss trial.

Switch trials are those where participants would want to avoid the terminating state from the previous trial. For example, participants should want to switch their choice if they picked the gray door on the last trial, went to the heist state, and the next trial is a loss trial. These trials comprised the following: (1) trials where they previously reached the heist state and the current trial was a loss trial; and (2) trials where they previously reached the neutral state and the current trial was a gain trial.

For both repeat and switch trials, the outcome on the previous trial can be positive or negative. For instance, while a participant ought to want to repeat the selection of a gray door if that took them to the heist state on the last trial and the next trial is a gain trial, the outcome on the last trial (when they went to the heist state) could have been positive or negative, depending on whether the last trial was a gain or a loss trial. Hence, we then further divided each trial type (repeat, switch) into those where they received a positive (+1 on gain trials, 0 on loss trials) or negative (-1 on gain trials, 0 on loss trials) outcome at the end of the

previous transition. This gave us four types of trials: repeat positive, repeat negative, switch positive, and switch negative. We calculated the percentage of trials that participants repeated or switched choices (as appropriate) for these four trial types for each participant. We then calculated a consistency score for positive trials by averaging together repeat positive and switch positive. We also did the same for negative trials.

For the behavioral experiment dataset, all trials were used. In the fMRI dataset, only free-choice trials were included (but transition sequences from the previous trial could be from a free or a force trial). Participants' consistency scores for positive were compared with negative using paired sample *t* tests (two tailed). First, we did this collapsing over contexts and conditions. This meant that the previous trial could have either been from the same or from the alternate context. Note that participants were not explicitly told of the conditions (i.e., whether to ignore or take notice of contextual cues) in the behavioral dataset. Although they were told this in the fMRI version of the task this ought not to bias this analysis. Nonetheless, we also repeated this analysis only using trials in the dependent condition.

Finally, we calculated each participant's outcome valence effect as the difference between consistency scores for positive trials (i.e., repeat positive and switch positive trials) minus consistency scores for negative trials (i.e., repeat negative and switch negative trials). This indexed the degree to which participants updated state transitions preferentially following positive compared with negative outcomes over both types of trials. We then correlated each participant's valence effect with their parametric betas extracted for the interaction regressor ( $|\delta|*$  outcome) from GLM1.

Data availability. Behavioral data and analysis scripts for all analyses are available at: https://github.com/summerfieldlab/Garrett\_Glitz\_etal. fMRI data (second-level SPM maps and similarity scores in regions of interest) are available at: https://osf.io/zvkj3/.

## Results

## Task and design

Participants (n = 29) performed a planning task in an fMRI scanner (the heist task; Fig. 1a). The task was introduced to participants via a cover story that suggested they were a burglar involved in a heist at one of four contexts, each denoted by a unique colored gem. Each trial occurred in one of these four (gem) contexts, and the relevant colored gem icon remained on the screen throughout the trial to make this clear. After trial onset, participants chose one of two doors (light vs dark), which were respectively associated in context c with probabilities  $p_c$  of transitioning to the (high-stakes) "heist" state and  $1 - p_c$  of transitioning to the "neutral" state (Fig. 1b).  $p_c$  switched randomly between 0.2 and 0.8 across the course of the experiment, meaning that a door was always likely to transition to one of the outcome states and unlikely to transition to the other. Participants were told that the transitions could change but were not told that there were two possible values that p could assume, what these values were, or how often the value of p could change.

Before making their choice, participants were presented with an additional cue that signaled whether, in the heist state, the participant would be caught (signaled by police cue; incurring a loss) or commit a successful burglary (signaled by swag cue; incurring a gain), whereas no positive or negative outcomes occurred in the neutral state (outcome of zero). The optimal policy was thus to learn the transition probability to approach the heist state in the presence of the swag cue and avoid the heist state in the presence of the police cue. To decorrelate choices and probabilities for the scanner, 75% of trials were "forced" in which only a single door was available, but in which transition probabilities could still be updated on receipt of reward. In the remaining 25% of trials, participants could freely choose between the two

doors. Participants were unaware during the initial door presentation whether the trial would be forced or free choice and therefore needed to actively consider transition probabilities on every trial.

The task was performed in alternating blocks that we label "dependent" and "independent" conditions. In dependent blocks, the transition probabilities associated with the two contexts (e.g.,  $p_1$  and  $p_2$ ) were yoked so that  $p_1 = p_2$  at all times (Fig. 1c). In independent blocks, the transition probabilities associated with the other two contexts (e.g.,  $p_3$  and  $p_4$ ) were unrelated (overlapping on average half of the time; Fig. 1d). The two contexts that made up each condition were randomly interleaved within a block, but the dependent and independent conditions themselves occurred in temporally distinct blocks of trials. Participants were told before starting the task about the two conditions and were told at the start of each new block whether they were entering a dependent or independent condition block (see Materials and Methods for full details about the task).

#### Behavioral analysis

We first asked whether behavior differed between the dependent and independent conditions. If participants generalized knowledge of the transition structure across contexts, then they should be more prone to use learning from context j to inform subsequent decisions in context i when in the dependent rather than the independent condition (note that this behavior is expected because participants were instructed about the dependence or independence among transition probabilities for the two gems in each block).

We used a logistic mixed-effects regression to measure this effect in a trial history-dependent fashion, asking how choices made on each trial t in context i depended on the history of state transitions observed over the previous five trials that had occurred in the contexts i and j, where j was the alternate context within the relevant condition (dependent or independent). To conduct this analysis, we recoded choices in a single frame of reference that removed the choice inversion between trials where police and swag cues were present. This was necessary because in our task, the transition history is relevant not for determining the specific response (light vs dark door), but rather the choice contingent on the presence of the swag or police cue. We call the historic information that is predictive of this recoded choice "transition evidence."

The results are shown in Figure 2. In the dependent condition, transition evidence from the previous two trials significantly predicted choice, both when it was experienced in the same  $[t - 1: fixed-effect \beta (95\% CI) = 1.11 (0.76-1.46); SE = 0.18;$ p < 0.001; t - 2:  $\beta = 0.43$  (0.17–0.70); SE = 0.13; p < 0.001) and when it was experienced in the alternate context to the current trial  $[t-1: \beta = 0.72 (0.42-1.02); SE = 0.15; p < 0.001; t-2: \beta =$ 0.40 (0.17–0.63); SE = 0.12; p < 0.001; Fig. 2a]. In contrast, in the independent condition, choices were only influenced by transition evidence when this was accrued in the same context (Fig. 2b). This was the case going one, two, three, and four trials back [t-1]:  $\beta = 0.62 \ (0.24-1.00); \ SE = 0.19; \ p = 0.001; \ t - 2: \ \beta = 0.30 \ (0.04-1.00); \ SE = 0.19; \ p = 0.001; \ t - 2: \ \beta = 0.30 \ (0.04-1.00); \ SE = 0.19; \ p = 0.001; \ t - 2: \ \beta = 0.30 \ (0.04-1.00); \ SE = 0.19; \ p = 0.001; \ t - 2: \ \beta = 0.30 \ (0.04-1.00); \ SE = 0.19; \ p = 0.001; \ t - 2: \ \beta = 0.30 \ (0.04-1.00); \ SE = 0.19; \ p = 0.001; \ t - 2: \ \beta = 0.30 \ (0.04-1.00); \ SE = 0.19; \ p = 0.001; \ t - 2: \ \beta = 0.30 \ (0.04-1.00); \ SE = 0.19; \ p = 0.001; \ t - 2: \ \beta = 0.30 \ (0.04-1.00); \ SE = 0.19; \ p = 0.001; \ t - 2: \ \beta = 0.30 \ (0.04-1.00); \ SE = 0.19; \ p = 0.001; \ t - 2: \ \beta = 0.30 \ (0.04-1.00); \ SE = 0.19; \ p = 0.001; \ t - 2: \ \beta = 0.30 \ (0.04-1.00); \ SE = 0.19; \ p = 0.001; \ t - 2: \ \beta = 0.30 \ (0.04-1.00); \ SE = 0.19; \ p = 0.001; \$ 0.55); SE = 0.13; p = 0.02; t - 3:  $\beta$  = 0.35 (0.09–0.61); SE = 0.13; p = 0.008; t - 4:  $\beta = 0.32$  (0.07–0.58); SE = 0.13; p = 0.01]. When transition evidence was accrued in the alternate context, this did not influence participants' subsequent choices, even on the immediately previous (t-1) trial  $[\beta = 0.07 (-0.12 \text{ to } 0.27);$ SE = 0.10, p = 0.47].

To directly compare the relative weight participants placed on past evidence received from the same and alternate contexts in each of the two conditions (dependent, independent), we ran an additional mixed-effects model. We computed the difference in transition evidence between the two contexts (averaged over the past five trials; we call this "differential evidence") for each condition (dependent/independent) and their interaction as predictors in this model. This revealed a significant interaction between differential evidence and condition  $[\beta = -0.41 \ (-0.63 \ \text{to} \ -0.18);$ SE = 0.11, p < 0.001 along with a main effect of differential evidence [ $\beta = 0.43$  (0.20–0.66); SE = 0.12, p < 0.001], but no main effect of condition [ $\beta = -0.05$  (-0.13 to 0.04); SE = 0.04, p = 0.27]. The interaction between differential evidence and condition remained significant in a permutation test that guards against greater similarity of feedback (in the dependent condition compared with the independent condition) confounding the effect  $(\beta = -0.41; 95\% \text{ range under the null distribution, } -0.25 \text{ to}$ 0.08; p < 0.001). Together, these results suggest that the relative preference for information received from the same (vs the alternate) context shifted between conditions. This was a result of participants increasing integration of information from the alternate context in the dependent condition.

We also analyzed data from an additional pilot experiment (n = 31; see Materials and Methods) with an identical structure except for the following two important differences: first, there were no forced-choice trials, and second, participants were not instructed about the dependence or independence of the transition structure but were left to discover it for themselves. In contrast to the fMRI cohort, in the independent condition, choices were influenced by transition evidence that accrued in both the same context  $[t - 1: \beta \ (95\% \ CI) = 1.20 \ (0.95-1.45); SE = 0.13;$ p < 0.001; t - 2:  $\beta = 0.65$  (0.49–0.82); SE = 0.08; p < 0.001; t - 3:  $\beta = 0.39 \ (0.26 - 0.52); SE = 0.07; p < 0.001; t - 4: \beta = 0.25 \ (0.15 - 0.001); t - 4: \beta = 0.25 \ (0.15$ 0.34); SE = 0.05; p < 0.001; t - 5:  $\beta = 0.19$  (0.09–0.29); SE = 0.05; p < 0.001] and in the other context  $[t - 1: \beta = 0.22 (0.07 - 0.37);$ SE = 0.08; p = 0.004; t - 2:  $\beta = 0.15$  (0.06-0.24); SE = 0.05; p = 0.001; t - 3:  $\beta = 0.10$  (0.002–0.20); SE = 0.05; p = 0.046; t - 4:  $\beta = 0.09 \ (0.004-0.179); \ SE = 0.04; \ p = 0.04; \ t - 5: \ \beta = 0.09$ (-0.001 to 0.19); SE = 0.049; p = 0.05]. Examining whether differential evidence interacted with condition revealed a significant interaction between differential evidence and condition [ $\beta$  = -0.097 (-0.17 to -0.02); SE = 0.04; p = 0.010]; however, this was not significant in the permutation test [ $\beta$  (95% range under the null distribution) = -0.097 (-0.25 to 0.08); p = 0.92]. As discussed below, potentially these results suggest that in the absence of instruction, participants may have a stronger prior that if two contexts (gems) co-occur in time, they belong to a shared latent context.

#### Computational model

Our modeling framework assumed that choices were determined by a mixture of associations learned in an independent and dependent fashion across contexts. We note at the outset that our model is not intended primarily as an account of the computations that humans undertake, but as an analytic tool that compactly parameterizes human policy with just a few parameters, which allows us to verify the degree to which humans share a model between contexts.

The model is composed of two learners, one that learns a shared transition function across a pair of contexts and another that learns a separate transition function for each context. On each trial, choices are determined by linearly mixing the estimated probabilities from each learner according to a weighting parameter, w, and using the resulting probabilistic estimate  $\hat{p}_c$  to compute the relative expected value of heist and neutral states,

Table 1. Model fitting and parameters

		Free					
	L00cv scores	parameters	β	$\alpha$	w (fixed)	w (dependent condition)	w (independent condition)
Fixed model	47.47 (±1.26)	3	1.80 (95% CI = 1.4–2.20)	0.65 (95% CI = 0.4–0.80)	0.61 (95% CI = 0.49-0.70)		
Flexible model	46.32* (±1.47)	3	1.59 (95% CI = 1.2–1.95)	0.56 (95% CI = 0.3-0.73)		0.85 (95% CI = 0.66-0.95)	0.15 (95% CI = 0.05-0.34)

The table summarizes for each model its fitting performances and its average parameters.  $\alpha$ , learning rate;  $\beta$ , softmax slope (sensitivity to the difference in the value of choosing dark vs light door on free-choice trials); w, weighting parameter (governs the weighted combination of context independent and context dependent transition functions). Data for model parameters are expressed as the mean and 95% confidence intervals (calculated as the sample mean  $\pm$  1.96  $\times$  SE).

according to which a choice was made via inverse temperature parameter  $\beta$ . The optimal policy (for an omniscient agent) would be to use w = 1 in the dependent condition and w = 0 in the independent condition. On each trial, participants updated the context-specific and the context-independent transition functions according to a state prediction error,  $\delta$ , which quantifies the degree of surprise at reaching a state given the option chosen and current estimates of the transition function.  $\delta$  was also weighted by w and the degree of update governed by a learning parameter,  $\alpha$ . Our rationale for modeling the learning of transitions as an incremental process (rather than beliefs fluctuating between p = 0.2 and p = 0.8) is that we did not explicitly instruct participants that there were two levels of p, what these levels were, or how often they could change. We assume that learning this underlying structure in practice would therefore be difficult (because of the stochasticity of the transitions, the existence of four different contexts, the frequency with which transitions change and the heist state fluctuating between gains and losses), but caution that alternate learning models could be used to formally test this assumption.

We compared two versions of this learning model. A fixed model in which w was held constant across the experiment was compared with a flexible model in which w was allowed to reverse between experimental conditions (i.e.,  $w_{\rm independent} = 1 - w_{\rm dependent}$ ). This feature of the flexible model gives it the capacity to shift between relying to a greater degree on separate transition functions in the independent condition (i.e., w toward 0) and relying on a shared transition function in the dependent condition (i.e., w toward 1). See Materials and Methods for full model specification.

## Flexible model adapts information integration between conditions

We fit each model to single-subject choices on a per-trial basis and compared fixed and flexible models by computing unbiased marginal likelihoods via subject-level leave-one-out cross-validation (LOOcv) for each participant. Comparison of LOOcv scores revealed significantly lower scores (indicating superior performance in cross-validation at predicting participant choices) for the flexible model compared with the fixed model ( $t_{(28)} = 2.72$ , p < 0.01, paired sample t test; Table 1, model parameters and LOOcv scores). Twenty-one of the 29 subjects (72% of subjects) were predicted better (had lower LOOcv scores) with the flexible model compared with the fixed model.

The best-fitting w parameter tended toward 1 in the dependent condition and 0 in the independent condition, consistent with the behavioral data. This indicates that participants learned a single transition function in dependent blocks but reverted to learning two different transition functions in independent blocks (by contrast, when w was held fixed across blocks, it assumed an intermediate value of  $\sim$ 0.61). A flexible model with two separate w parameters (one per condition, fitted separately) did not

account any better for participant choices than the flexible model with a single w that reversed between conditions ( $t_{(28)} = -1.59$ , p = 0.12). Simulating choices using a population of subjects drawn according to best-fitting parameters of the flexible model showed that the flexible model qualitatively recapitulated the change in relative preference for information from the alternate versus the same context between conditions (Fig. 2a,b) to a greater degree than choices simulated from the fixed model (Fig. 2c,d).

#### Neuroimaging data

Having established that participants behave differently in the dependent and independent conditions, we turned to the fMRI data to understand the neural mechanisms that supported this differential behavior. Our goal was to use multivariate approaches (including RSA) to examine how multivoxel patterns encoding transition probabilities (i.e., beliefs about the forthcoming state) were related in the dependent and independent conditions. However, we first adopted a univariate analysis to identify target sites for the coding of the state transition function, using the SPE from the model. We expected that the MTL would be sensitive to SPEs, consistent with a long tradition implicating the hippocampus in the formation of state associations (Eichenbaum et al., 1999), and a detector of states that either match or violate the agent's expectations (Kumaran and Maguire, 2007; Duncan et al., 2012).

#### Univariate analysis

We thus modeled BOLD responses at the time the transitioned-to state (heist or neutral) was revealed using a parametric predictor encoding the unsigned state prediction error  $|\delta|$  extracted from the flexible model. This analysis collapsed over conditions (dependent, independent). This modulator was included along-side other quantities coding for outcome, trial type (forced/free choice), and the interaction of outcome and  $|\delta|$  (see Materials and Methods).

The BOLD signal correlated negatively with  $|\delta|$  in two MTL clusters [peak left (x, y, z): -20, -4, -28;  $t_{(28)} = 5.01$ ; p < 0.001 uncorrected for multiple comparisons; peak right: 18, -4, -21;  $t_{(28)} = 4.22$ ; p < 0.001 uncorrected), which survived a small volume correction using a bilateral anatomical MTL mask [peak left: -20, -7, -24;  $t_{(28)} = 5.01$ ; FWE corrected at the peak level within bilateral MTL mask  $(p_{\rm FWE}) = 0.008$ ; peak right: 18, -4, -21;  $t_{(28)} = 4.22$ ;  $p_{\rm FWE} = 0.047$ ]. In total, 10.14% of voxels lay within the anatomically defined amygdala, 33.33% within the hippocampus, 49.28% within the parahippocampus, and 5.80% in the entorhinal cortex (Fig. 3a), determined by assessing overlap with anatomical masks generated in WFU pickatlas (see Materials and Methods).

The negative direction of the parametric effect indicates a greater change in BOLD response to expected (compared with unexpected) state transitions. We combined these clusters (extracted at p < 0.001 uncorrected) into a single bilateral functional ROI

<sup>\*</sup>p < 0.01 comparing LOOCV scores between the two models (paired sample t test). Lower scores indicate superior performance in cross-validation.

mask (Fig. 3b), which we then used for subsequent multivariate analyses.

#### Representational similarity analysis

Next, we used a multivariate approach to assess the mapping from BOLD responses in our functional ROI to transition probabilities, and to measure how this mapping changed over contexts. We began with an analysis of BOLD signals at the time of choice (i.e., when the door was presented). This is the time point during which participants needed to consider the transition probability to each prospective second-level state. We first used RSA, measuring the correlation distance across multivoxel patterns associated with transition probabilities p (heist state | door presented) derived from our flexible learning model into quartiles, both across blocks and across gems (Fig. 3c). Note that our prediction is that neural patterns encoding transition probabilities should be more similar across contexts in dependent than in independent blocks. We thus computed a similarity score by averaging correlations in diagonal (same probability quartile) versus off-diagonal (different probability quartile) cases, separately for the two contexts in the dependent and independent conditions.

This revealed a significant condition (dependent, independent)  $\times$  quartile (diagonal, off-diagonal) interaction ( $t_{(28)} = 4.02$ ; p < 0.001; 95% CI, 0.11–0.33; paired sample t test). This was the result of a difference in similarity between on-diagonal and off-diagonal scores in the dependent condition ( $t_{(28)} = 5.33$ ; p < 0.001; 95% CI, 0.11–0.26; one-sample t test vs 0), which was absent in the independent condition ( $t_{(28)} = -0.82$ ; p = 0.42; 95% CI, –0.11 to 0.05; one-sample t test vs 0; Fig. 3d).

One interpretation of this finding is that in the dependent condition, the MTL encodes the state transition function for each context with a common neural pattern. However, we also considered some alternative possibilities. First, we examined whether the results held if we allocated trials to bins using fixed probabilities across the unity range (i.e., quartile 1, 0.00-0.25; quartile 2, 0.26–0.50; quartile 3, 0.51–0.75; quartile 4, 0.76–1.00) rather than adapting bins for each participant according to the specific distribution of probabilities they used. This revealed the same pattern of results (condition \* diagonal interaction:  $t_{(28)} = 4.20$ ; p < 0.001; 95% CI, 0.10–0.30; difference in similarity between on-diagonal and off-diagonal bins in the dependent condition:  $t_{(28)} = 5.73$ ; p < 0.001; 95% CI 0.13–0.28; difference in similarity between on-diagonal and off-diagonal bins in the independent condition:  $t_{(28)} = 0.04$ ; p = 0.97; 95% CI, -0.07 to 0.08). Second, we checked that the number of trials in each probability quartile were well matched between contexts, finding that they were  $(t_{(28)} = 1.50; p = 0.55; 95\% \text{ CI}, -0.02 \text{ to } 0.15)$ . Finally, we were concerned that the effect might arise as a spurious effect of closer temporal proximity between trials in the same transition probability quartile in dependent blocks. To address this, first we checked whether the average difference between the temporal distance of trials in on-diagonal versus off-diagonal quartile combinations was correlated with the difference in representational similarity (see Materials and Methods). This was neither the case in the dependent condition (r = -0.20, p = 0.32) nor the independent condition (r = 0.15, p = 0.44).

We then repeated our analysis in cross-validation across sessions. In other words, we measured the similarity between quartile/bin  $n_i$  and  $n_j$ , where i and j are drawn from different scanner runs, and computed the average for each similarity bin across all possible  $c_{1j}$  and  $c_{2j}$  combinations, where  $i \neq j$ . This revealed the same (albeit weaker) pattern of results with fixed probability bins (condition \* diagonal interaction:  $t_{(28)} = 2.04$ ; p = 0.05; 95% CI, -0.00 to 0.06) and probability quartiles ( $t_{(28)} = 1.89$ ; p = 0.069;

95% CI, -0.00 to 0.07). Finally, we repeated this cross-validation analysis, this time comparing similarity scores within the same context (separately for each condition). Contrary to what we had expected, this did not reveal a significant difference in either condition (dependent condition:  $t_{(28)} = 1.09$ ; p = 0.29; 95% CI, -0.01 to 0.03; independent condition:  $t_{(28)} = 0.42$ ; p = 0.68; 95% CI, -0.01 to 0.02; paired *t* tests comparing on-diagonal with off-diagonal similarity scores). In other words, while we were able to successfully decode probabilities between contexts in cross-validation in the dependent condition, this was not the case within context (for either condition). We caution that this does question the robustness of the between-context RSA. Reassuringly however, we also did not observe the condition \* diagonal interaction we had observed for the between-context case ( $t_{(28)} = -0.53$ ; p = 0.60; 95% CI, -0.03 to 0.02). Furthermore, we did not find evidence to suggest that decoding was stronger for the between-context RSA compared with the within-context RSA in the dependent condition ( $t_{(28)} = -0.69$ ; p = 0.49, paired t test comparing the difference in on-diagonal and off-diagonal similarity scores within vs between contexts), an effect that would have been at odds with participants using a shared transition model. Comparing scores between conditions also revealed a weak effect in the direction we would predict under the hypothesis that participants would switch to use of a context-specific model in the independent condition with the difference in decoding accuracy being greater for the within-context versus the between-context RSA in the independent condition compared with the dependent condition [ $t_{(28)} = 1.69$ , p(one tailed) = 0.05].

## Multivariate encoding model

Next, taking a complementary approach, we built an encoding model that mapped transition probabilities [in the frame of reference p(state = heist|door presented) derived from the flexible learning model as before] flexibly onto voxels within the MTL ROI, separately for each context  $c_a$ . We then inverted this model to predict transition probabilities both for the same context  $c_a$  and the other three (held out) contexts (contexts)  $c_b$ , where  $a \neq b$  (Fig. 3e, schematic of this analysis). This approach allowed us to train and test in cross-validation, by obtaining weights from session (scanner run) *i* and then using these to predict the probabilities for each context on session j. The model output was a  $4 \times 4$  (context  $\times$  context) matrix of predicted versus true (model-derived) transition probabilities, which we compared via cross-entropy loss. This allowed us to measure whether, within the MTL, neural patterns coding for probabilities were more similar across contexts in the dependent condition (e.g.,  $c_1 \rightarrow c_2$ and  $c_2 \rightarrow c_1$ ) than in the independent condition (e.g.,  $c_3 \rightarrow c_4$ and  $c_4 \rightarrow c_3$ ). Unlike the RSA approach, this also allowed us to compare two different coding schemes. It could either be the case that state associations are encoded in a high-dimensional format in which probabilities map onto bins with no input structure. This can be implemented via a one-hot input function in the encoding model, which also enables us to test various levels of granularity of binning, to verify that the RSA results were not specific to our choice of having four bins. Alternatively, it could instead be the case that probabilities are encoded in a lowdimensional format, whereby neural patterns are more similar for closer probabilities (e.g., bin 1 is more similar to bin 2 than to bin 4). This can be implemented via a Gaussian input function (effectively, a tuning curve for probability) in the encoding model. Probabilities were converted to odds ratios for this exercise (see Materials and Methods).

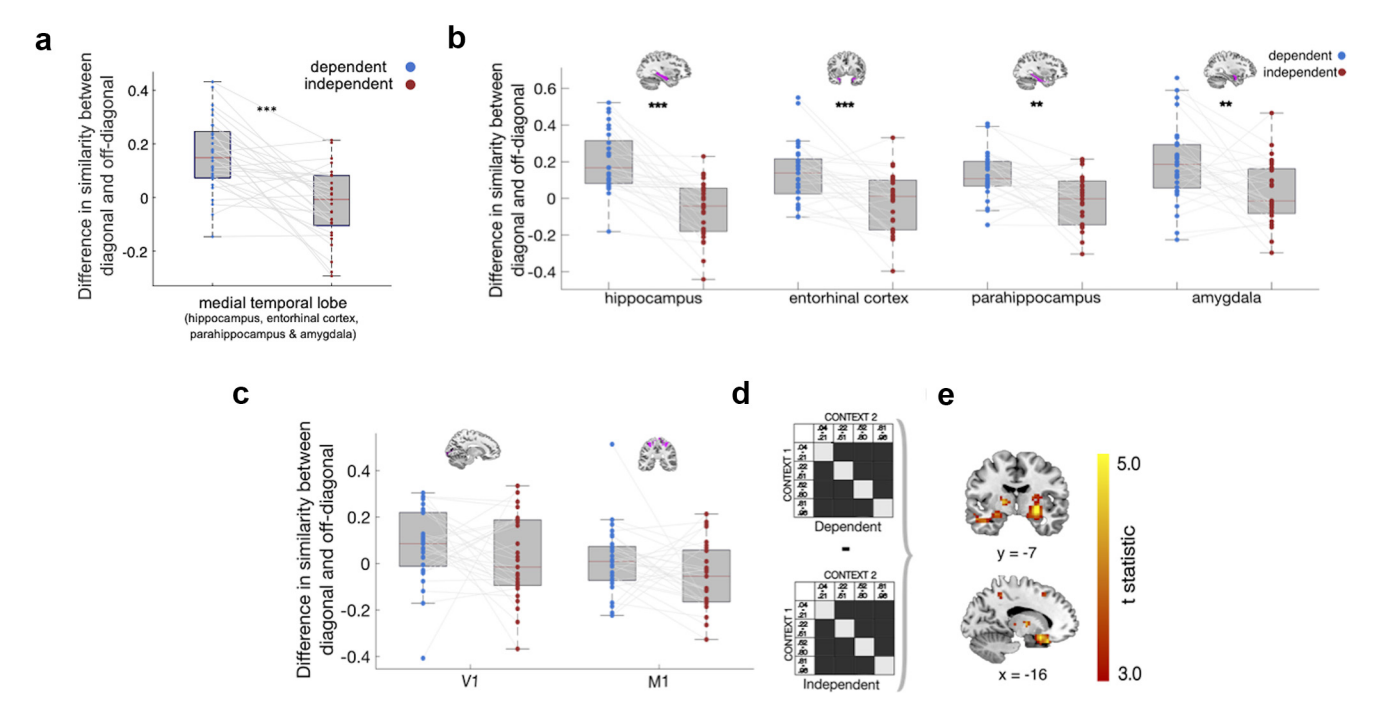


**Figure 4.** a-c, RSA in Figure 3c was repeated using a anatomical mask of the entire MTL (a) and subregions of the MTL (b), specifically, bilateral hippocampus, parahippocampus, entorhinal cortex, and amygdala, as well as in V1 and M1 (control regions; c). d, Illustration of the whole-brain searchlight interaction analysis; the difference between on-diagonal and off-diagonal similarity was contrasted between conditions. c, Whole-brain searchlight interaction analysis revealed greater similarity between on-diagonal versus off-diagonal in the dependent condition compared with the independent condition in our functional ROI, right dorsal striatum (top panel) and left IFG/OFC (bottom panel). Brain images shown at p < 0.001 uncorrected, thresholded at t > 3. Error bars show SEM. \*significant at p < 0.05; \*\*significant at p < 0.01; \*\*\*significant at p < 0.001.

The results validated and extended those of the RSA. Using one-hot encoding of probability, we found stronger evidence of shared encoding of probability in the dependent condition compared with the independent condition. Furthermore, this effect was independent of the number of bins chosen, as long as there were >3 bins (Fig. 3f). We obtained the most robust effects with ~6 bins (implying a psychologically plausible granularity to the estimation of transition probabilities), for which the crossvalidated loss was substantially higher between contexts in the independent condition than those in the dependent condition  $(t_{(28)} = -3.12, p = 0.002)$ . When cross-validation was performed across sessions only, reconstructing both probabilities in the other context as well as in the same context using information from another session (e.g.,  $c_1$ session1  $\rightarrow c_1$ session2), we found the same pattern of results ( $t_{(28)} = -3.80$ ; p < 0.001). Similar results were also obtained at different granularities. Interestingly, we were unable to recreate these effects under the additional constraint imposed by Gaussian encoding of probability ratios. This implies that while there is a consistent code for transition probabilities, its similarity structure does not map smoothly onto the one-dimensional axis given by probability.

# Replication of results using anatomical ROI of the medial temporal lobe

To investigate whether the effects we observed were specific to our choice of functional ROI, we conducted a subsequent RSA. This was exactly as described above (for between contexts), only this time we used voxels from a bilateral anatomical MTL mask comprising four subregions of the MTL, specifically hippocampus, parahippocampus, entorhinal cortex, and amygdala. Replicating the effects we observed in our functional ROI, this revealed a significant condition (dependent, independent)  $\times$  quartile (diagonal, off-diagonal) interaction ( $t_{(28)} = 5.23$ ; p < 0.001; 95% CI,

0.11–0.25; paired sample t test; Fig. 4a). This was the result of a difference in similarity between on-diagonal and off-diagonal scores in the dependent condition ( $t_{(28)} = 6.12$ ; p < 0.001; 95% CI, 0.10–0.21; one-sample t test vs 0), which was absent in the independent condition ( $t_{(28)} = -0.96$ ; p = 0.345; 95% CI, -0.07 to 0.03). We also observed the same pattern of results (i.e., cross-validated loss substantially higher between contexts in the independent condition than the dependent condition) rerunning the multivariate encoding model using this anatomical ROI in place of the functional ROI (four-bin case:  $t_{(28)} = -2.85$ ; p = 0.02; six-bin case:  $t_{(28)} = -3.23$ ; p = 0.002).

# Characterizing the nature of the effect in the medial temporal lobe

Next, to investigate whether the observed effects were specific to particular subregions of the MTL, we conducted four further RSAs on voxels using separate anatomical masks for each of the four MTL subregions (hippocampus, parahippocampus, entorhinal cortex, and amygdala). Fisher transformed similarity scores were then entered into a region  $\times$  condition (dependent/independent) 4\*2 repeated-measures ANOVA. This revealed a main effect of condition ( $F_{(1,28)}=29.40$ ; p<0.001) with the difference in similarity (M) between on-diagonal and off-diagonal scores greater in the dependent than independent condition ( $M_{\rm hippocampus}=0.26$ ,  $M_{\rm parahippocampus}=0.13$ ,  $M_{\rm entorhinal\ cortex}=0.15$ ,  $M_{\rm amygdala}=0.16$ ) as well as a region  $\times$  condition interaction ( $F_{(2,45.68.54)}=3.91$ ; p=0.018; Greenhouse–Geisser corrected).

To better understand the interaction, we proceeded to test the difference in similarity scores between conditions in each region with every other region (correcting for multiple comparisons). This revealed a larger difference between conditions in the hippocampus compared with each of the other three MTL subregions (entorhinal cortex, amygdala, and parahippocampus; all

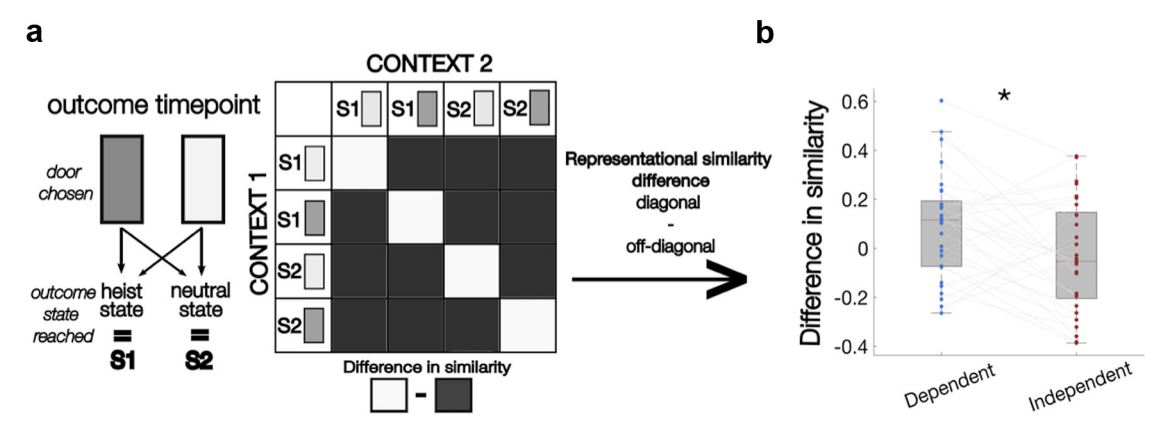


**Figure 5. a**, RSA at trial outcome. We examined the BOLD similarity at the time of outcome between matched choice (door)—outcome state combinations and mismatched combinations between contexts in the two conditions. **b**, In our MTL ROI, the difference between representational similarity of matched and mismatched combinations was significantly greater in dependent than independent blocks. Error bars show SEM. \*significant at p < 0.05.

p < 0.05, paired sample t test) with the parahippocampus surviving correction for multiple comparisons ( $t_{(28)}$  = 3.91; p = 0.001, significant at Bonferroni-corrected threshold of p < 0.008). There was also a main effect of region ( $F_{(3,84)}$  = 3.33; p = 0.023), with the difference across both conditions being significantly greater in the amygdala than in both parahippocampus ( $t_{(28)}$  = 3.07; p = 0.005) and entorhinal cortex ( $t_{(28)}$  = 2.81; p = 0.009). Together, these results suggest that greater similarity in transition encoding in the dependent compared with the independent condition was not exclusive to a particular subregion of the MTL but was most pronounced in the hippocampus (Fig. 4a).

Finally, to test whether the differences between our conditions were selective to the MTL or present over the whole brain, we conducted the same RSA using voxels in the following two control regions: early visual cortex (V1) and primary motor cortex (M1). There was no significant difference between conditions in either control region (V1:  $t_{(28)} = -0.28$ ; p = 0.78; 95% CI, -0.08 to 0.06; M1:  $t_{(28)} = -0.22$ ; p = 0.83; 95% CI, -0.09 to 0.08; Fig. 4c).

#### RSA whole-brain searchlight

Next, we repeated the same RSA as described above across the whole brain using a searchlight approach. In the dependent condition, this identified activity within our functional ROI (right peak: 22, -7, -18;  $t_{(28)}\!=\!4.31$ ; FWE corrected at peak level within functional ROI mask,  $p_{\rm FWE}=0.005$ ; left peak: -24, -7, -18;  $t_{(28)}\!=\!4.92$ ; FWE corrected at peak level within functional ROI mask,  $p_{\rm FWE}=0.001$ ). The cerebellum also survived familywise error correction for multiple comparisons at the cluster level (cluster-defining threshold,  $p\!<\!0.001$ , uncorrected). We did not find any evidence for differences in similarity in or outside our functional ROI in the independent condition, even at very lenient thresholds ( $p\!<\!0.01$  uncorrected).

Next, we conducted a new searchlight that directly tested the difference in similarity for on-diagonal versus off-diagonal bins between conditions (Fig. 4*d*). This also revealed activation in our functional ROI (right peak: 22, -7, -18;  $t_{(28)} = 3.55$ ; FWE corrected at peak level within functional ROI mask,  $p_{\rm FWE} = 0.02$ ; left peak: -27, -10, -14;  $t_{(28)} = 4.02$ ; FWE corrected at peak level within functional ROI mask,  $p_{\rm FWE} = 0.006$ ). A cluster in the right dorsal striatum (29, -7, -7:  $t_{(28)} = 5.80$ ; p < 0.001, FWE cluster-level corrected; Fig. 4*e*), which extended into the hippocampus, as well as the inferior frontal gyrus (IFG) adjacent to Brodmann area 47 (-16, 14, -18:  $t_{(28)} = 5.08$ ; p = 0.007) and left cerebellum

(-2, -46, -21:  $t_{(28)}$  = 4.92; p = 0.03) also survived familywise error correction for multiple comparisons over the whole brain at the cluster level (cluster-defining threshold, p < 0.001 uncorrected).

## Multivariate analysis during transition probability updating

The analyses described so far focus on the time point when planning takes place (door presentation). What happens during updating? To examine this, we conducted a related analysis at the time of transition outcome (i.e., when participants learned whether, conditional on their choice, they had reached the heist or the neutral state). We reasoned that to update the state-action representations appropriately (in a shared or unshared manner across contexts) it would be necessary to re-encode both the selected action (light vs dark door) and encountered state (heist vs neutral). We thus partitioned data according to these factors and investigated whether BOLD signals were more similar when both state and action matched (i.e., on-diagonal elements) versus where they did not (off-diagonal elements) at the time of updating, separately for the dependent and independent conditions (Fig. 5a) in our functional ROI. This analysis also revealed a significant condition  $\times$  diagonal interaction ( $t_{(28)} = 2.67$ ; p = 0.01; 95% CI, 0.03–0.22; paired sample t test; Fig. 5b), driven by a significant difference in similarity between matched and mismatched choice-state combinations (Fig. 5a, on vs off diagonal) in the dependent condition ( $t_{(28)} = 2.35$ ; p = 0.03; 95% CI, 0.01– 0.18; one-sample t test vs 0) which was absent in the independent condition ( $t_{(28)} = -0.78$ ; p = 0.44; 95% CI, -0.12 to 0.05).

Once again, this effect was not specific to a particular subregion of the MTL. We entered similarity scores from RSAs conducted in subregions of the MTL into a condition (dependent, independent) by region (hippocampus, parahippocampus, entorhinal cortex, amygdala) ANOVA. This revealed a main effect of condition ( $F_{(1,27)} = 10.05$ ; p = 0.004). There was no main effect of region ( $F_{(3,81)} = 0.95$ ; p = 0.42) or region  $\times$  condition interaction ( $F_{(3,81)} = 1.21$ ; p = 0.31). There was no difference between conditions in two control brain regions (V1:  $t_{(28)} = 1.16$ ; p = 0.26; 95% CI, -0.04 to 0.16; M1:  $t_{(28)} = 1.66$ ; p = 0.11; 95% CI, -0.02 to 0.15). Finally, a whole-brain searchlight comparing the difference in similarity scores between on-diagonal and off-diagonal between conditions revealed a significant interaction within our state prediction error ROI (left: -16, -4, -32;  $t_{(28)} = 3.47$ ; p = 0.02, cluster level corrected within our SPE mask), as well as in a

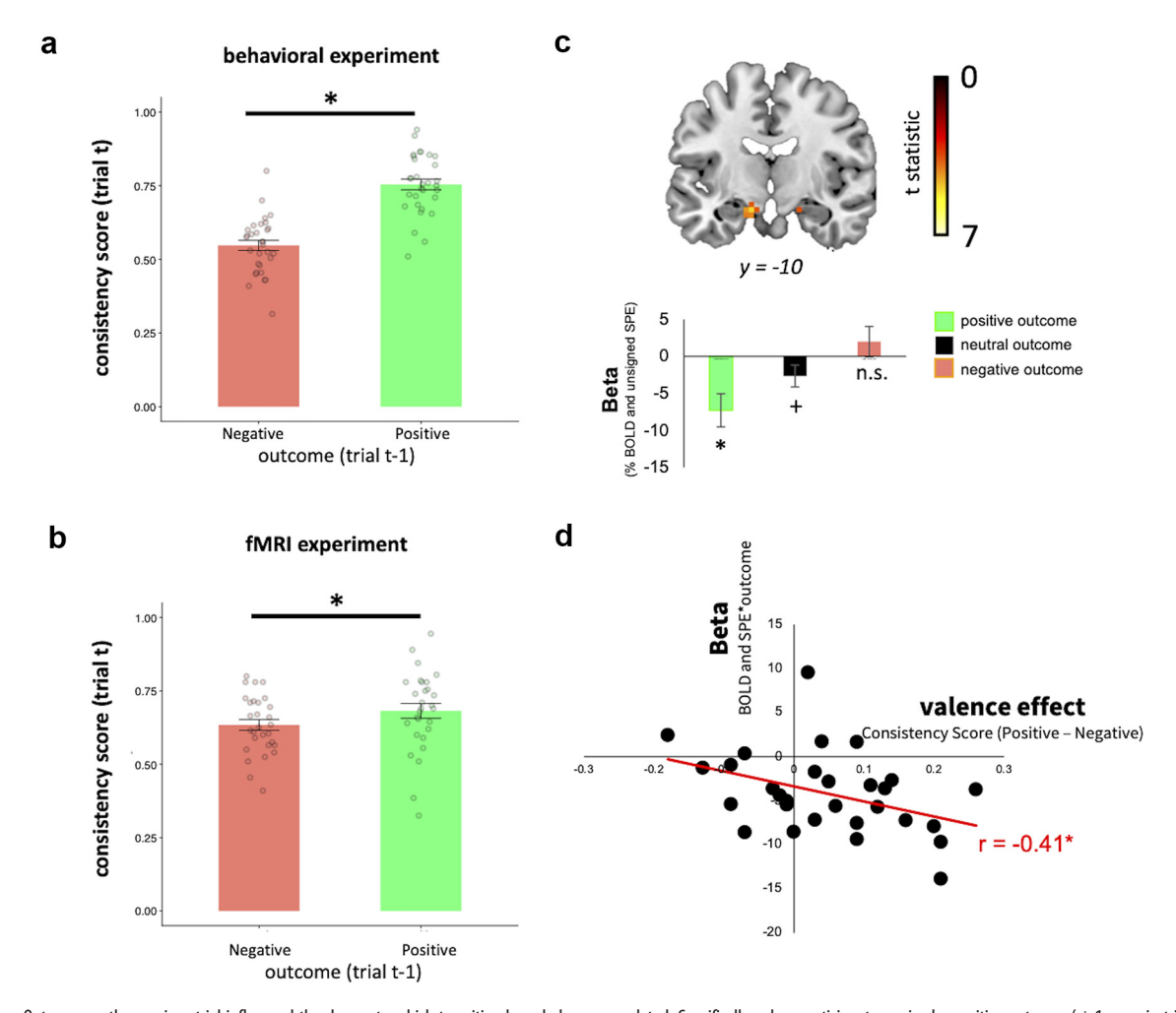


**Figure 6.** Outcome on the previous trial influenced the degree to which transition knowledge was updated. Specifically, when participants received a positive outcome (+1 on gain trials or 0 on loss trials), consistency scores (indexed as the percentage of repeat choices for desirable trials and the percentage of switch choices for undesirable trials) were higher compared with when they received a negative outcome. a, b, This was observed in participants who completed a behavioral study outside the scanner (a) and our fMRI cohort (b). c, Unsigned state prediction errors were modulated by outcome valence in the MTL [peak (x, y, z): -13, -10, -18; t<sub>(28)</sub> = 4.87; p = 0.018, FWE whole-brain cluster level corrected]; image displayed at p < 0.001 uncorrected. a, The magnitude of the valance effect observed behaviorally (quantified as green minus red in a) correlated with the size of the interaction betas observed in the fMRI data in a0 (Spearman's a0 = 0.41, a1, a2, a3, a3, a4, a5, a5, a6, a6, a7, a8, a8, a9, a9,

cluster composed of right hippocampus extending into pons  $(t_{(28)} = 5.05; p < 0.0001, uncorrected; 12, 18, -18; <math>p = 0.04$ , cluster level corrected across the whole brain with cluster-forming threshold of p < 0.001 uncorrected). No other significant effects were observed.

#### Outcome valence modulates updating of state transitions

An interesting feature of our design is that the transition function changes (with reversals of p) in a way that is unrelated to outcomes. This means that, in theory, any learning about the transition function should not depend on whether the outcome was positive or negative. To test whether participants might be biased to update the transition function more or less according to the outcome, we calculated a consistency score (see Materials and Methods) for each participant. This measured the consistency of each choice given transitions experienced on the previous trial. A high consistency score indicates that a participant updates transitions strongly on the basis of feedback. This was calculated separately for trials in which participants received a positive outcome (+1 on a gain trials or 0 on a loss trial) and those in which they received a negative outcome (-1 on a loss trial or 0 on a gain trial) on the previous trial. Notably, this is not the

same as a win–stay, lose–switch bias, as a choice would be considered consistent only if it considered both past transitions and the current reward/loss incurred when reaching the heist state (i.e., if choosing the dark door on trial t-1 had resulted in monetary gain, but the current trial t was a police trial (monetary loss), the consistent choice would be to choose the light door on trial t).

We first conducted this analysis in a separate behavioral experiment (described as "pilot" above; n = 31; see Materials and Methods). This experiment included exclusively free-choice trials, giving us greater power to be able to detect valence effects. In this version of the task, participants were not told about any structure between contexts and integrated information from each context in each condition.

Participants integrated evidence from the other context in the dependent condition (1–4 trials back) in this dataset but also did so in the independent condition; therefore, we remain agnostic as to whether participants adjusted how they integrated feedback from state transitions between the two conditions and primarily use this dataset to examine how outcome interacts with learning the state transitions. This revealed that transition updating was greater following positive compared with negative outcomes  $(t_{(30)} = 9.79; p < 0.001, paired sample t test; Fig. 6a)$ . In other

words, participants updated state transition knowledge and adjusted their subsequent behavior to a greater degree when outcomes were positive compared with negative. Note that this analysis collapses over contexts (see Materials and Methods). However, the main effect remains ( $t_{(30)} = 8.14$ ; p < 0.001) when we run this same analysis restricted to the dependent condition.

Next, we ran the same analysis on our fMRI participants (restricted to free-choice trials; Fig. 6b). We again observed a main effect of outcome with greater updating following positive outcomes compared with negative outcomes ( $t_{(28)} = 2.24$ ; p = 0.03). This effect remained when analysis was restricted to trials from the dependent condition ( $t_{(28)} = 2.60$ ; p = 0.015).

In two datasets, our participants' behavior suggested that rewards received influenced the degree to which the transition function was updated with a greater update following positive compared with negative outcomes. If this is the case, we would predict that SPE signals in the MTL, which drive updates to the transition function, ought to be larger following positive outcomes compared with negative. To test this, we examined the interaction of the unsigned state prediction error regressor and outcome in a univariate whole-brain analysis (controlling for the main effects of each; see Materials and Methods). This revealed a negative effect in a cluster in the left MTL [peak (x, y, z): -13, -10, -18; p = 0.018, whole-brain FWE cluster level corrected after thresholding at p < 0.001], which included voxels within our functional ROI [peak (x, y, z): -16, -7, -18; t<sub>(28)</sub> = 4.08; small volume corrected using functional ROI mask]. No other regions survived whole-brain correction. Note that since the main effect of SPE is also negative (Fig. 3a), the sign of this interaction suggests a greater parametric effect of unsigned SPEs in the MTL following positive versus negative outcomes.

Finally, we examined whether there was a relationship between this interaction effect in the MTL (i.e., the degree to which unsigned SPEs were modulated by outcome valence) and participants' behavior (the degree to which consistency scores were greater for positive outcomes compared with negative outcomes). We quantified each participant's behavioral outcome valence effect (Fig. 6b) by taking the difference in consistency scores between positive and negative outcomes and correlated these with each participants parametric SPE \* outcome interaction  $\beta$  (this quantifies the degree to which the parametric effect of unsigned SPEs are modulated by outcome). This revealed a negative correlation that was robust to outliers (Spearman's  $\rho = -0.41$ ; p < 0.03); specifically, the greater participants showed a bias toward integrating information following transition sequences that ended in a positive outcome (vs negative) in their choices, the greater the extent to which unsigned SPEs expressed in the MTL were greater for higher (vs lower) outcomes.

## **Discussion**

We studied the neural and computational mechanisms by which humans combine or segment information about the transition structure of the world. For the fMRI experiment, we chose to directly instruct our participants, as our hypothesis was agnostic to whether model sharing occurred because of instruction or trial-and-error learning. Consequently, our computational model is an analytic tool and does not offer a process-level account of model sharing. Previous structure learning tasks have suggested that participants are able to use the similarity of latent variables such as value estimates, prediction errors, and their covariation over time to draw links between different contexts (Acuña and Schrater, 2010; Wunderlich et al., 2011). Bayesian inference

models in which latent causes are inferred and used to group together experiences (Gershman and Niv, 2010; Gershman et al., 2015; Niv, 2019; Sanders et al., 2020) could also be a means by which participants learn to group different contexts together in practice. Another possibility is that neural geometry actively represents the relational organization of task elements (Luyckx et al., 2019; Bernardi et al., 2020; Sheahan et al., 2021). However, our encoding model did not find a smoothly varying relationship between neural coding and probability, which seems like it would follow naturally from such a representation.

To address the question of how neural population activity encoded transition probabilities within and between contexts, we began by identifying voxels that responded differentially according to whether a transition between states was expected or unexpected, using estimates of SPEs to parameterize this effect. We found that responses to SPEs correlated with BOLD responses in brain regions that overlapped with the bilateral hippocampus (Fig. 3a). Of note, the parametric effect of SPEs in the MTL were negative. This might seem surprising given the past implication of the (more anterior) hippocampus in novel or surprising stimuli (Strange et al., 2005). We speculate that such a signal might occur, however, if internal representations were strengthened following evidence that confirms prior beliefs.

We first focused our analysis on voxels in this region and measured the consistency in neural patterns in these voxels in encoding transition probabilities between conditions. First, we adopted an RSA-based method to show that the encoding of probability was more similar across contexts in the dependent condition than the independent condition. We caveat that we were not able to decode probabilities within context using this same approach and caution that this challenges the robustness of this analysis. It may be that there is a confound that gives rise to between-context decoding that leaves within-context decoding unaffected, or that the identical gem features present when decoding within gem (e.g., color, shape of each gem) make decoding transition probabilities more difficult or better suited to a different RSA than we use for the between-context case (e.g., dividing probability into a different number of bins rather than four quartiles). Other explanations could also give rise to this discrepancy. Comparing the difference in within-context and between-context decoding between conditions yielded a pattern (albeit weakly and with due caution with respect to the possibility of a type I error) of results in line with what we would expect. Namely, that the difference in within-context versus betweencontext decoding was stronger in the independent compared with the dependent condition, consistent with a switch between context-specific and context-nonspecific models.

Next, we adopted a more flexible encoding modeling pipeline as a complementary multivariate approach. This told a similar story: that the brain learned a representation that was similar across contexts when this was beneficial, but partitions probability encoding into different patterns when it is necessary to disambiguate the predictions for different contexts. The encoding model also enabled us to examine the pattern of results under two different coding schemes: a Gaussian input function and a one-hot input function. Interestingly, while the one-hot input function replicated the pattern of RSA and was robust to the range of different probability bins being used, the Gaussian input function did not. We are not entirely clear about why this is the case. Previous theories have emphasized that neural populations in cortex may encode probability distributions in smoothly varying ways, permitting forms of function approximation or Bayesian inference (Ma et al., 2006; Orhan and Ma,

2017), and there is even some support for this class of theory from studies involving BOLD recordings (Van Bergen et al., 2015). However, the nature of the coding scheme for transition probabilities in hippocampus remains unclear. Future work could potentially develop this encoding model approach to examine whether other task variables influence the representational structure encoded in the hippocampal formation [e.g., the level of uncertainty in beliefs, priors, anticipatory (state) prediction errors, and the degree to which predictions diverge for different actions].

Observing these effects in the MTL is consistent with past findings that have identified the involvement of the MTL in learning state associations (Miyashita, 1988; Eichenbaum et al., 1999; Schapiro et al., 2012, 2013; Deuker et al., 2016; Garvert et al., 2017; Yokose et al., 2017; Rey et al., 2018), encoding relational knowledge that can be used to generalize and draw inferences across contexts (Bunsey and Eichenbaum, 1996; Wimmer and Shohamy, 2012; Zeithamova et al., 2012; Kumaran et al., 2016; Koster et al., 2018; Park et al., 2019) and its role in modelbased planning (Bradfield et al., 2020), including in similar twostage sequential planning tasks (Miller et al., 2017; Vikbladh et al., 2019) potentially via the representation of task structure (Geerts et al., 2020). Our initial analysis focused on a region that included different subregions of the MTL. But when we repeated our RSA approach separately in 4 different anatomical subregions of the MTL-hippocampus, entorhinal cortex, amygdala, and parahippocampus—we found a significant effect in each of these (an effect that was absent in two control regions). This is suggestive that a network of MTL regions is involved in encoding the predictive relationships between states necessary for planning—consistent with past findings using a paradigm similar to ours (Boorman et al., 2016)—and that each component in this network has the capacity to flexibly adapt the representations it uses to facilitate the sharing of models between contexts when prudent to do so. The involvement of a number of subregions might account for why disabling a specific part of the MTL does not always lead to reductions in goal-directed behavior (Corbit and Balleine, 2000; Gaskin et al., 2005). Interestingly, the effect we observed was strongest in bilateral hippocampus, in line with its involvement in modulating pattern separation between contexts and memories via inputs from other MTL brain regions including the entorhinal cortex (Yassa and Stark, 2011). However, future work, ideally with higher-resolution fMRI or direct recordings, is needed to help characterize the precise functional contribution of each of these subregions.

We also examined whether there were other regions of the brain in which representations had a similar selective pattern similarity between contexts by running a whole-brain searchlight analysis. In addition to confirming the involvement of the MTL, this detected a strong effect in the dorsal striatum and the left IFG. This analysis was exploratory, and neither of these brain regions was hypothesized to be involved from the outset. While the IFG and adjacent orbitofrontal cortex (OFC) have previously been shown to be involved in inferring task states using fMRI multivariate approaches (Schuck et al., 2016; Niv, 2019), the striatum was particularly unexpected given its well established role in model-free learning (Montague et al., 1996; Joel et al., 2002; O'Doherty et al., 2004; Geerts et al., 2020), although (and with the necessary caveats with regard to retrospective inference) there is some evidence from fMRI and lesion studies that the dorsal striatum, along with prefrontal cortex (Niv, 2009; Balleine and O'Doherty, 2010), may also play an important role in model-based planning behavior (Yin et al., 2005a,b), though exactly what the functional role that either region fulfills here in the service of our task is unclear.

Examining participants' stay/switch behavior revealed an effect of valence whereby, following positive outcomes, participants updated transition probabilities to a greater degree than following negative outcomes. We note that these findings are unlikely to be accounted for by purely model-free state-action learning since our task and updating metric includes cases where participants should (if using model-based control and updating the transition function) repeat choices following negative outcomes and switch choices following positive outcomes. These cases would cancel out the effect of valence that we actually observe in the data under a model-free controller (which would repeat following positive outcomes and switch following negative outcomes). An effect of valence on updating was also observed in the fMRI data, which revealed a greater parametric effect of SPEs for positive outcomes relative to negative outcomes in the MTL. Interestingly, this pattern of asymmetric updating is reminiscent of confirmation bias (Nickerson, 1998), a recent account of which (Lefebvre et al., 2022) has shown that this learning asymmetry can in fact be beneficial by driving apart the difference in value between the different options. Future theoretical work may help shed light on whether a similar normative account exists behind the asymmetry we observe here in planning.

Together, these results shed important light on the computational processes by which the MTL maintains and adapts knowledge about the consequences of our choices and actions in the world. By relying on a common representational code, knowledge can be shared across different contexts that we interact with.

#### References

Acuña DE, Schrater P (2010) Structure learning in human sequential decision-making. PLoS Comput Biol 6:e1001003.

Balleine BW, O'Doherty JP (2010) Human and rodent homologies in action control: corticostriatal determinants of goal-directed and habitual action. Neuropsychopharmacology 35:48–69.

Baram AB, Muller TH, Nili H, Garvert MM, Behrens TEJ (2021) Entorhinal and ventromedial prefrontal cortices abstract and generalize the structure of reinforcement learning problems. Neuron 109:713–723.e7.

Bernardi S, Benna MK, Rigotti M, Munuera J, Fusi S, Salzman CD (2020) The geometry of abstraction in the hippocampus and prefrontal cortex. Cell 183:954–967.e21.

Bezanson J, Karpinski S, Shah VB, Edelman A (2012) Julia: a fast dynamic language for technical computing. arXiv:1209.5145.

Boorman ED, Rajendran VG, O'reilly JX, Behrens TE (2016) Two anatomically and computationally distinct learning signals predict changes to stimulus-outcome associations in hippocampus. Neuron 89:1343–1354.

Bradfield LA, Leung BK, Boldt S, Liang S, Balleine BW (2020) Goal-directed actions transiently depend on dorsal hippocampus. Nat Neurosci 23:1194–1197.

Bunsey M, Eichenbaum H (1996) Conservation of hippocampal memory function in rats and humans. Nature 379:255–257.

Canto CB, Wouterlood FG, Witter MP (2008) What does anatomical organization of entorhinal cortex tell us? Neural Plast 2008;381243.

Charpentier CJ, Moutsiana C, Garrett N, Sharot T (2014) The brain's temporal dynamics from a collective decision to individual action. J Neurosci 34:5816–5823.

Corbit LH, Balleine BW (2000) The role of the hippocampus in instrumental conditioning. J Neurosci 20:4233–4239.

Daw ND, Gershman SJ, Seymour B, Dayan P, Dolan RJ (2011) Model-based influences on humans' choices and striatal prediction errors. Neuron 69:1204–1215.

Deuker L, Bellmund JL, Schröder TN, Doeller CF (2016) An event map of memory space in the hippocampus. Elife 5:e16534.

Doll BB, Duncan KD, Simon DA, Shohamy D, Daw ND (2015) Model-based choices involve prospective neural activity. Nat Neurosci 18:767–772.

- Duncan K, Ketz N, Inati SJ, Davachi L (2012) Evidence for area CA1 as a match/mismatch detector: a high-resolution fMRI study of the human hippocampus. Hippocampus 22:389–398.
- Eichenbaum H, Dudchenko P, Wood E, Shapiro M, Tanila H (1999) The hippocampus, memory, and place cells: is it spatial memory or a memory space? Neuron 23:209–226.
- Garrett N, Daw ND (2020) Biased belief updating and suboptimal choice in foraging decisions. Nat Commun 11:12.
- Garrett N, Lazzaro SC, Ariely D, Sharot T (2016) The brain adapts to dishonesty. Nat Neurosci 19:1727–1732.
- Garvert MM, Dolan RJ, Behrens TE (2017) A map of abstract relational knowledge in the human hippocampal–entorhinal cortex. Elife 6:e17086.
- Gaskin S, Chai SC, White NM (2005) Inactivation of the dorsal hippocampus does not affect learning during exploration of a novel environment. Hippocampus 15:1085–1093.
- Geerts JP, Chersi F, Stachenfeld KL, Burgess N (2020) A general model of hippocampal and dorsal striatal learning and decision making. Proc Natl Acad Sci U|S|A 117:31427–31437.
- Gershman SJ, Niv Y (2010) Learning latent structure: carving nature at its joints. Curr Opin Neurobiol 20:251–256.
- Gershman SJ, Norman KA, Niv Y (2015) Discovering latent causes in reinforcement learning. Curr Opin Behav Sci 5:43–50.
- Gläscher J, Daw N, Dayan P, O'Doherty JP (2010) States versus rewards: dissociable neural prediction error signals underlying model-based and model-free reinforcement learning. Neuron 66:585–595.
- Huys QJ, Cools R, Gölzer M, Friedel E, Heinz A, Dolan RJ, Dayan P (2011)
  Disentangling the roles of approach, activation and valence in instrumental and pavlovian responding. PLoS Comput Biol 7:e1002028.
- Joel D, Niv Y, Ruppin E (2002) Actor–critic models of the basal ganglia: new anatomical and computational perspectives. Neural Netw 15:535–547.
- Juechems K, Balaguer J, Ruz M, Summerfield C (2017) Ventromedial prefrontal cortex encodes a latent estimate of cumulative reward. Neuron 93:705–714.e4.
- Kleiner M, Brainard D, Pelli D (2007) What's new in Psychtoolbox-3? Perception 36:1–16.
- Koster R, Chadwick MJ, Chen Y, Berron D, Banino A, Düzel E, Hassabis D, Kumaran D (2018) Big-loop recurrence within the hippocampal system supports integration of information across episodes. Neuron 99:1342– 1354.e6.
- Kumaran D, Maguire EA (2007) Match-mismatch processes underlie human hippocampal responses to associative novelty. J Neurosci 27:8517–8524.
- Kumaran D, Banino A, Blundell C, Hassabis D, Dayan P (2016) Computations underlying social hierarchy learning: distinct neural mechanisms for updating and representing self-relevant information. Neuron 92:1135–1147.
- Lancaster JL, Woldorff MG, Parsons LM, Liotti M, Freitas CS, Rainey L, Kochunov PV, Nickerson D, Mikiten SA, Fox PT (2000) Automated Talairach atlas labels for functional brain mapping. Hum Brain Mapp 10:120, 131
- Lefebvre G, Summerfield C, Bogacz R (2022) A normative account of confirmation bias during reinforcement learning. Neural Computationm 34:307–337.
- Luyckx F, Nili H, Spitzer B, Summerfield C (2019) Neural structure mapping in human probabilistic reward learning. Elife 8:e42816.
- Ma WJ, Beck JM, Latham PE, Pouget A (2006) Bayesian inference with probabilistic population codes. Nat Neurosci 9:1432–1438.
- Maldjian JA, Laurienti PJ, Kraft RA, Burdette JH (2003) An automated method for neuroanatomic and cytoarchitectonic atlas-based interrogation of fMRI data sets. Neuroimage 19:1233–1239.
- Miller KJ, Botvinick MM, Brody CD (2017) Dorsal hippocampus contributes to model-based planning. Nat Neurosci 20:1269–1276.
- Miyashita Y (1988) Neuronal correlate of visual associative long-term memory in the primate temporal cortex. Nature 335:817–820.
- Montague PR, Dayan P, Sejnowski TJ (1996) A framework for mesencephalic dopamine systems based on predictive Hebbian learning. J Neurosci 16:1936–1947.
- Nickerson RS (1998) Confirmation bias: a ubiquitous phenomenon in many guises. Rev Gen Psychol 2:175–220.
- Nili H, Wingfield C, Walther A, Su L, Marslen-Wilson W, Kriegeskorte N (2014) A toolbox for representational similarity analysis. PLoS Comput Biol 10:e1003553.

- Niv Y (2009) Reinforcement learning in the brain. J Math Psychol 53:139–154.
- Niv Y (2019) Learning task-state representations. Nat Neurosci 22:1544– 1553.
- O'Doherty J, Dayan P, Schultz J, Deichmann R, Friston K, Dolan RJ (2004) Dissociable roles of ventral and dorsal striatum in instrumental conditioning. Science 304:452–454.
- Orhan AE, Ma WJ (2017) Efficient probabilistic inference in generic neural networks trained with non-probabilistic feedback. Nat Commun 8:14.
- Park SA, Miller DS, Nili H, Ranganath C, Boorman ED (2019) Map making: constructing, combining, and navigating abstract cognitive maps. bioRxiv. doi: 10.1101/810051.
- Rey HG, De Falco E, Ison MJ, Valentin A, Alarcon G, Selway R, Richardson MP, Quiroga RQ (2018) Encoding of long-term associations through neural unitization in the human medial temporal lobe. Nat Commun 9:4372.
- Sanders H, Wilson MA, Gershman SJ (2020) Hippocampal remapping as hidden state inference. Elife 9:e51140.
- Schapiro AC, Kustner LV, Turk-Browne NB (2012) Shaping of object representations in the human medial temporal lobe based on temporal regularities. Curr Biol 22:1622–1627.
- Schapiro AC, Rogers TT, Cordova NI, Turk-Browne NB, Botvinick MM (2013) Neural representations of events arise from temporal community structure. Nat Neurosci 16:486–492.
- Schuck NW, Cai MB, Wilson RC, Niv Y (2016) Human orbitofrontal cortex represents a cognitive map of state space. Neuron 91:1402–1412.
- Sheahan H, Luyckx F, Nelli S, Teupe C, Summerfield C (2021) Neural state space alignment for magnitude generalization in humans and recurrent networks. Neuron 109:1214–1226.e8.
- Strange BA, Hurlemann R, Duggins A, Heinze HJ, Dolan RJ (2005) Dissociating intentional learning from relative novelty responses in the medial temporal lobe. Neuroimage 25:51–62.
- Sutton RS, Barto AG (1998) Introduction to reinforcement learning. Cambridge, MA: MIT.
- Tootell RB, Hadjikhani NK, Vanduffel W, Liu AK, Mendola JD, Sereno MI, Dale AM (1998) Functional analysis of primary visual cortex (V1) in humans. Proc Natl Acad Sci U|S|A 95:811–817.
- Tzourio-Mazoyer N, Landeau B, Papathanassiou D, Crivello F, Etard O, Delcroix N, Mazoyer B, Joliot M (2002) Automated anatomical labeling of activations in SPM using a macroscopic anatomical parcellation of the MNI MRI single-subject brain. Neuroimage 15:273–289.
- Van Bergen RS, Ma WJ, Pratte MS, Jehee JF (2015) Sensory uncertainty decoded from visual cortex predicts behavior. Nat Neurosci 18:1728–1730.
- Vikbladh OM, Meager MR, King J, Blackmon K, Devinsky O, Shohamy D, Burgess N, Daw ND (2019) Hippocampal contributions to model-based planning and spatial memory. Neuron 102:683–693.e4.
- Wimmer GE, Shohamy D (2012) Preference by association: how memory mechanisms in the hippocampus bias decisions. Science 338:270–273.
- Wunderlich K, Symmonds M, Bossaerts P, Dolan RJ (2011) Hedging your bets by learning reward correlations in the human brain. Neuron 71:1141–1152.
- Wunderlich K, Dayan P, Dolan RJ (2012) Mapping value based planning and extensively trained choice in the human brain. Nat Neurosci 15:786–791.
- Yassa MA, Stark CE (2011) Pattern separation in the hippocampus. Trends Neurosci 34:515–525.
- Yin HH, Knowlton BJ, Balleine BW (2005a) Blockade of NMDA receptors in the dorsomedial striatum prevents action–outcome learning in instrumental conditioning. Eur J Neurosci 22:505–512.
- Yin HH, Ostlund SB, Knowlton BJ, Balleine BW (2005b) The role of the dorsomedial striatum in instrumental conditioning. Eur J Neurosci 22:513–523.
- Yokose J, Okubo-Suzuki R, Nomoto M, Ohkawa N, Nishizono H, Suzuki A, Matsuo M, Tsujimura S, Takahashi Y, Nagase M, Watabe AM, Sasahara M, Kato F, Inokuchi K (2017) Overlapping memory trace indispensable for linking, but not recalling, individual memories. Science 355:398–403.
- Zeithamova D, Dominick AL, Preston AR (2012) Hippocampal and ventral medial prefrontal activation during retrieval-mediated learning supports novel inference. Neuron 75:168–179.